# Chapter 4:
## The E3-ligase RNF26 regulates Myosin VI mediated endosomal positioning in interphase and mitotic cells

**M.L.M. Jongsma*, I. Berlin*, H. Janssen, F. Kleinpenning, P.A. van Veelen, G.M. Janssen, M.A. Garstka, L. Janssen and J. Neefjes**

*Manuscript in preparation*

**Most cells have a characteristic architecture with their various compartments localized at defined sites. The Trans-Golgi Network follows the Golgi and the majority of early and late endosomes cluster close to the microtubule organizing center. How the intracellular distribution is determined in cells and why this is important for cellular functioning, is unknown. Here we show how the RING-domain containing protein RNF26 acts as a master regulator of the intracellular positioning of the endosomal system. We show that RNF26 is localized in the Endoplasmic Reticulum membrane where it recruits the scaffolding proteins SQSTM1 or DOCK7. These scaffolding proteins are ubiquitinated leading to the recruitment of the adaptor proteins Tollip, Tom1L2, EPS15 and/or TAX1BP1 by their ubiquitin-binding motifs. In close proximity to RNF26, these adaptor proteins become ubiquitinated stabilizing their binding to the actin based motor Myosin VI which tethers adaptor protein-bound vesicles to actin filaments. Proper positioning of endosomes controlled by RNF26 is important for cells to allow proper cytokinesis.**



A visual inspection of cells shows a characteristic pattern of the various endosomal compartments. The nucleus is usually indented which defines the site of the microtubule organizing center (MTOC) that organizes the microtubule-cytoskeleton. Between the nucleus and the MTOC, usually the Golgi and Trans Golgi-Network (TGN) are located. Beyond the MTOC, most early and late endosomes accumulate in a cloud with other vesicles moving along the microtubules to and from the plasma membrane. The mitochondria and the Endoplasmic Reticulum (ER) fill the cytosolic space. These characteristic distributions are not random and thus have to be organized properly. How this is regulated is unclear.

Positioning and movement of intracellular vesicles and cellular organelles is controlled by motor proteins. Three types of motor proteins have been distinguished: kinesins, dyneins and myosins. Kinesins and dyneins drive long-distances transport along microtubules, while myosin motor proteins control short-range transport along actin filaments [1]. The interaction between motor proteins and their respective cargo has to be regulated. This is only partially understood but often involves characteristic small GTPases that either directly or via their effector proteins interact with different motor proteins. These interactions are subsequently controlled by processes like phosphorylation and ubiquitination, and by cholesterol in sometimes complex systems, as illustrated for late endosomal and lysosomal transport. The dynein-dynactin motor is recruited to late endosomes and lysosomes by the Rab7 effector Rab-interacting lysosomal protein (RILP) [2]. The cholesterol sensor ORP1L binds to the Rab7-RILP complex and can acquire two conformations dependent on the cholesterol content in the late endosomal or lysosomal membrane. Under high cholesterol conditions ORP1L binds cholesterol in the membrane, while the Rab7-RILP complex interacts with the dynein motor. Under low cholesterol conditions, the cholesterol-binding domain of ORP1L is released, thereby exposing its FFAT domain which interacts with an ER protein called VAMP-associated protein A (VAP-A). VAP-A then removes the dynein motor from the Rab7-RILP complex inhibiting transport [3]. The ER thus controls the movement of late endosomes and lysosomes. In fact, the ER has been defined to communicate with many cellular compartments such as the Golgi, mitochondria, endosomes, lysosomes and the plasma membrane [4,5]. This suggests that the concept of a single compartment orbiting in empty cellular space is incorrect. The cell contains many interactions between different compartments to allow intercompart-

ment control of movement, metabolomics and signaling. Here, we will provide another example of intercompartmental control, namely the control of endosomal positioning. The endocytic route, consisting of different endosome types, is a well-known cellular pathway in which regulated transport is highly important. Endosomes are thought to function as multifunctional platforms, transporting a unique set of membranes, proteins and assembled molecular machines to their specific cellular locations in space and time [6]. Therefore it is highly important for endosomes to be localized and thus transported properly. In a previously published genome wide siRNA-based screen we looked for proteins involved in endosomal transport [7] and we identified the protein RNF26, a potential E3-ligasewith a thus far unknown function, to play a role in this process. RNF26 appears to be a multi-pass RING domain containing ER localized protein controlling the correct positioning of all endosomal compartments, but not mitochondria, the ER or the Golgi complex. We identified potential RNF26 targets via GST-pulldown using its RING-domain containing tail. This way we identified the actin motor protein Myosin VI no insert isoform as a RNF26 interacting protein.

Myosin VI is an unconventional Myosin with a unique 53-aa insert between its motor domain and IQ motif, giving it the ability to transport cargo towards the minus-end of actin filaments [8]. Myosin VI has been shown to be a multi-functional motor protein. It has been found on different cellular locations and is involved in processes as endocytosis, autophagy and cytokinesis. Myosin VI is able to perform all these functions because it binds to a wide variety of proteins. Myosin VI is known to play a role in endocytosis, via its binding partners disabled-2 (Dab2) [9-11] and glucose-transporter binding protein (GIPC) [11,12]. The Myosin VI binding partners Optineurin, nuclear dot protein 52 (NDP52) and Tax1 binding protein 1 (TAX1BP1) all contain a LC3-interacting domain and have been shown to be present on autophagosomes. Together with its binding partner target of myb 1 (Tom1), Myosin VI has been shown to play a role in the delivery of endosomal membranes to autophagosomes by docking to optineurin, NDP52 and TAX1BP1 [13]. Although GIPC was originally described as a myosin VI interacting protein involved in endocytosis, it is also shown to play a role in Myosin VI regulated cytokinesis. Both Myosin VI and GIPC depletion results in an increase of multi-nucleated cells, which is an indication of improper cytokinesis [14]. Since myosin VI is involved in a wide variety of functions, it is important that Myosin VI is regulated and only becomes active in correct space and time in the cell. Beside Myosin VI, we also identified Toll interacting protein (Tollip), Tom1 like 2 (Tom1L2), TAX1BP1, Sequestosome 1 (SQSTM1), epidermal growth factor receptor pathway substrate 15 (EPS15) and dedicator of cytokinesis 7 (DOCK7) as RNF26 interacting proteins involved in the control of endosome localization. This list contains proteins that are already identified as Myosin VI interacting proteins, namely Tom1L2 [15], TAX1BP1 [16] and DOCK7 [17]. Here we show how the ER localized E3 ligase RNF26 controls the positioning of endosomal vesicles by controlling a signaling cascade involving the Guanine Exchange Factor DOCK7, an autophagy regulator SQSTM1, various adaptors specified by ubiquitin binding domains including the TGN receptor TAX1BP1 and the endosomal receptors EPS15, Tom1L2 and Tollip for the myosin motor Myosin VI. We show that proper endosomal positioning by this RNF26 controlled new signaling network is essential for proper cytokinesis.

**Results**

*RNF26 regulates the intracellular distribution*

*of endocytic compartments*

We have performed a siRNA-based Genome Wide screen for factors controlling MHC class II biology. For this analyses we performed flow cytometry, microscopy and qPCR to place hits in functional subgroups [7]. One candidate, the RING domain containing protein RNF26 showed an unique activity by microscopy as it altered the steady state distribution of different endosomal compartments; the late endosomal/lysosomal MHC class II compartments and recycling endosomes (labeled by HLA-DR and TfR). In these RNF26 depleted cells endosomes were no longer accumulating in the perinuclear area, but were instead found dispersed throughout the cytoplasm and frequently accumulated in the tips of cells (Figure 1A). This was confirmed in another cell line (In HeLa, Figure S1A). The dispersed phenotype in RNF26 depleted cells was confirmed and quantified in a deconvolution step using three single siRNA duplexes targeting RNF26 (Figure 1B). These duplexes silence RNF26 by 80% as determined by qPCR (Figure 1C). EEA1 positive Early Endosomes, CD63 positive late endosomes and TGN46 labeled Trans Golgi Network (in fact all components of the endosomal pathway) all lost their intracellular steady state distribution following depletion of RNF26 (Figure 1D). The localization of the Golgi, stained with Giantin and Golgin 97 and mitochondria, stained using mitotracker was not affected (Figure 1D and Figure S1B). These results suggest that RNF26 selectively controls the intracellular distribution of the entire endosomal pathway.

*RNF26 E3 ligase activity and ER-membrane localization are important for its function*

The C-terminal tail of RNF26 contains a C3HC5-RING domain (Figure 2A). Based on the RING-domain alignment of RNF26 with three other E3-ligase RING domains, we created two inactive RNF26 mutants (Figure 2B). We replaced Cystein-401 for a Serine (C401S) and in the second mutant Isoleucine-382 (known to be often involved in interactions with the E2) was mutated into an Arginine (I382R) [18]. To determine the activity of these two mutants, the rate of RNF26 auto-ubiquitination activity was determined by overexpressing RFP-RNF26 or its mutants along with HA-Ubiquitin followed by biochemistry. We isolated RNF26 and probed for ubiquitin. RNF26 C401S and RNF26 I382R showed a strongly reduced auto-ubiquitination signal when compared to wt RNF26, suggesting that the mutants are indeed inactive (Figure 2C). Besides its C-terminal RING domain, the N-terminus of RNF26 contains at least four (predicted) transmembrane domains (TMHMM Server v. 2.0). We found RNF26 localized in the ER membrane by confocal microscopy, showing co-localization with the ER proteins VAP-A and Unconventional SNARE in the ER 1 (USE1) (Figure S2A and B). ER localization of RNF26 was confirmed by Electron Microscopy using PDI as an ER marker (Figure 2D). Rescue experiments were performed to determine if the E3-ligase activity and/or the ER localization of RNF26 are essential for its role in endosome localization. While overexpression of full length active RNF26 rescued the late endosome dispersion phenotype, the inactive mutants RNF26 C401S and RNF26 I382R as well as overexpression of only the cytosolic tail of RNF26 could not (Figure 2E). This suggest that RNF26 ER localization and its E3-ligase activity are essential for the positioning of endosomes.

*Identification of RNF26 interacting proteins; A central role for the motor protein Myosin VI*

To further understand how the ER protein RNF26 controls endosomal positioning, we defined RNF26 interacting proteins by GST-pulldown, using both the soluble Tail (aa304-433) and the shorter RING-domain (aa363-433) of RNF26. Analysis by Mass

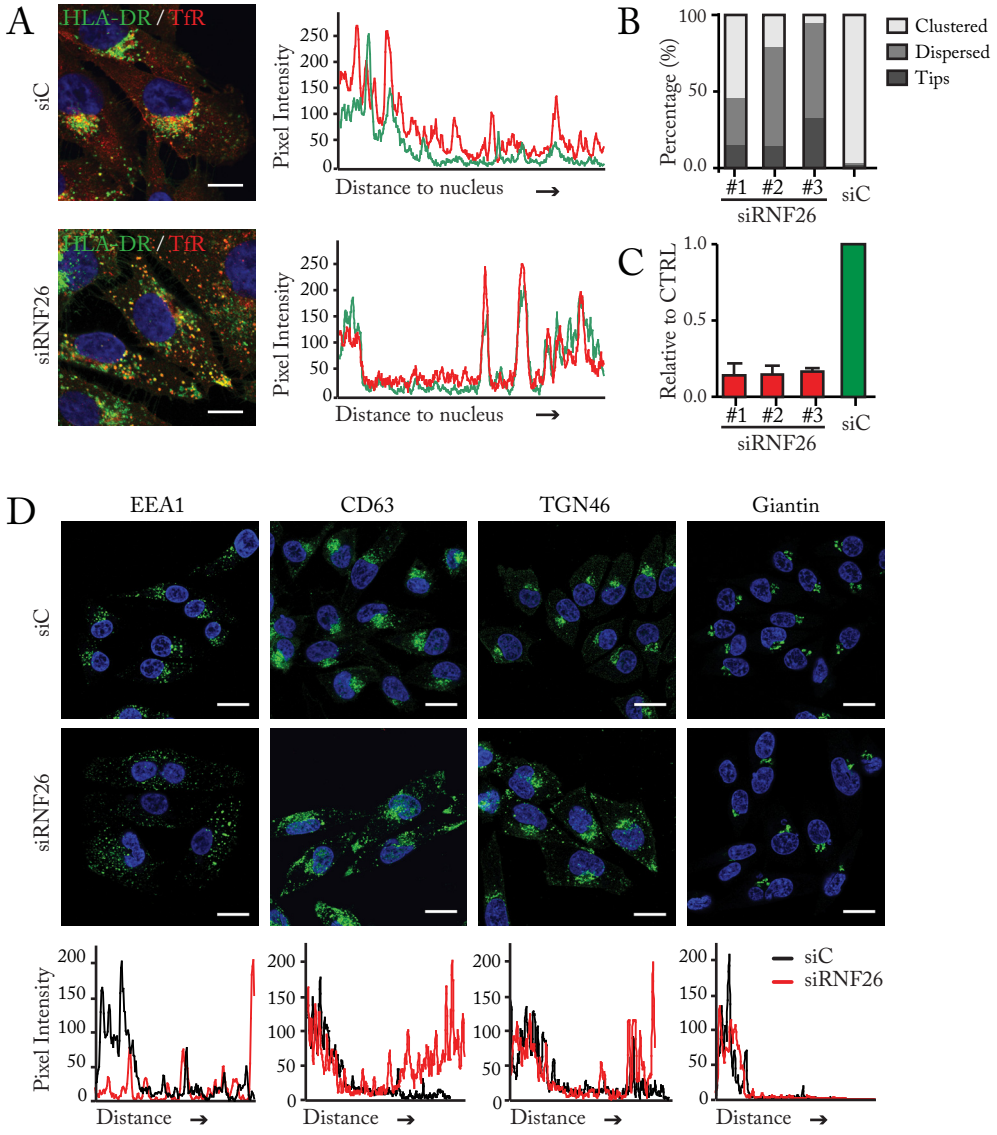


Figure 1 | **RNF26 regulates the intracellular distribution of endocytic compartments.** (A) MelJuSo cells depleted for RNF26 show dispersion of MHC class II (HLA-DR, green) and Transferrin Receptor (TfR, red) containing vesicles compared to cells transfected with a non-targeting siRNA duplex. The nucleus is stain using Hoechst (Blue). Pixel Intensity plots show the distance of the fluorescent signal relative to the nucleus in RNF26 silenced and control cells (HLA-DR, green; TfR, Red). (B) Quantification of the dispersion phenotype using three different siRNA duplexes targeting RNF26. (C) Silencing efficiency of the three different siRNA duplexes targeting RNF26 was measured by qPCR. All duplexes reduce RNF26 expression with 80% relative to the control. (D) MelJuSo cells depleted for RNF26 were stained for EEA1 (Early endosomes), CD63 (Late endosomes), TGN46 (Trans Golgi Network) and Giantin (Golgi). The nucleus was stained using Hoechst (Blue). Pixel intensity plots show the distance of the fluorescent signal relative to the nucleus (siC, black line; siRNF26, red line). Early endosomes, Late endosomes and the Trans Golgi Network have a dispersed distribution in RNF26 depleted cells while control cells show their clustering. The Golgi itself was not affected by RNF26 depletion. (Bar = 10μm)

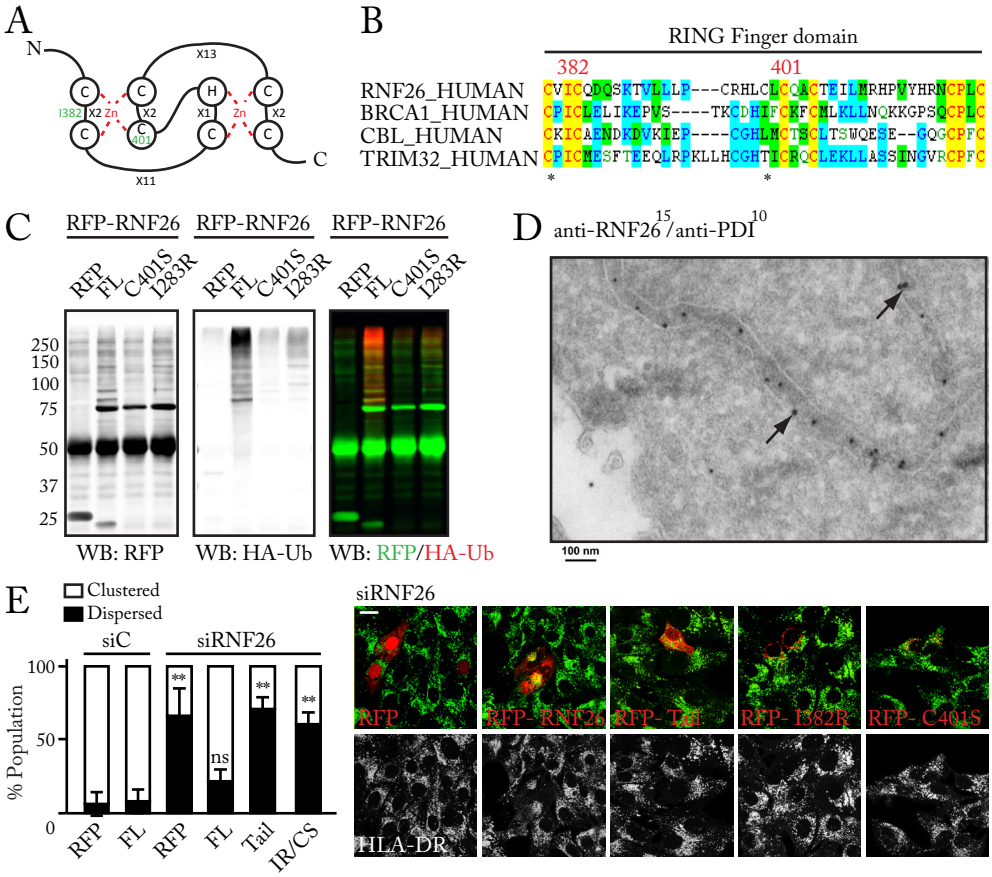


Figure 2 | **RNF26 E3 ligase activity and ER-membrane localization are important for its function.** (A) RNF26 contains a C3HC4 type RING domain. The localization of the amino acids mutated to create inactive mutants of RNF26 are depicted in green (I382 and C401). (B) Alignment of the RING domain of RNF26 and the well studied active RING domains of BRCA1, CBL and TRIM32. I382 and C401 are conserved between the different RING domains. (C) HEK293T cells overexpressing RNF26, RNF26 I382R, RNF26 C401R or empty vector in combination with HA-ubiquitin were immunoprecipitated for RFP-tagged RNF26 and analyzed by western blot. While RNF26 and the RNF26 mutants are expressed (left and green signal), HA-ubiquitin is clearly co-immunoprecipitated with full length RNF26 but the HA-ubiquitin signal is strongly reduced after overexpression of the RNF26 mutants suggesting inactivity of their RING domain (middle and red signal). (D) Electron microscopy was used to show RNF26 (15nm gold particles) localization in the ER membrane, which was stained by PDI (10nm gold particles). (E) RNF26 depleted cells were stained for MHC class II (HLA-DR). Overexpression of full length RNF26 rescued the endosomal dispersion phenotype, while expression of the Tail domain of RNF26 or the inactive RNF26 mutants I382R and C401S could not. (Bar = 10μm), **p<0.001

Spectometry led to the identification of 18 potential interacting proteins (Figure S3A and SB). To select for interacting proteins involved in endosomal positioning, we silenced all 18 candidates and determined whether they showed the endosomal dispersion phenotype observed in RNF26 depleted cells. Depletion of seven candidates, including the motor protein Myosin VI, resulted in endosomal dispersion (Figure 3A; quantification in Figure 3B). Silencing of these seven candidates was confirmed by Western blot-

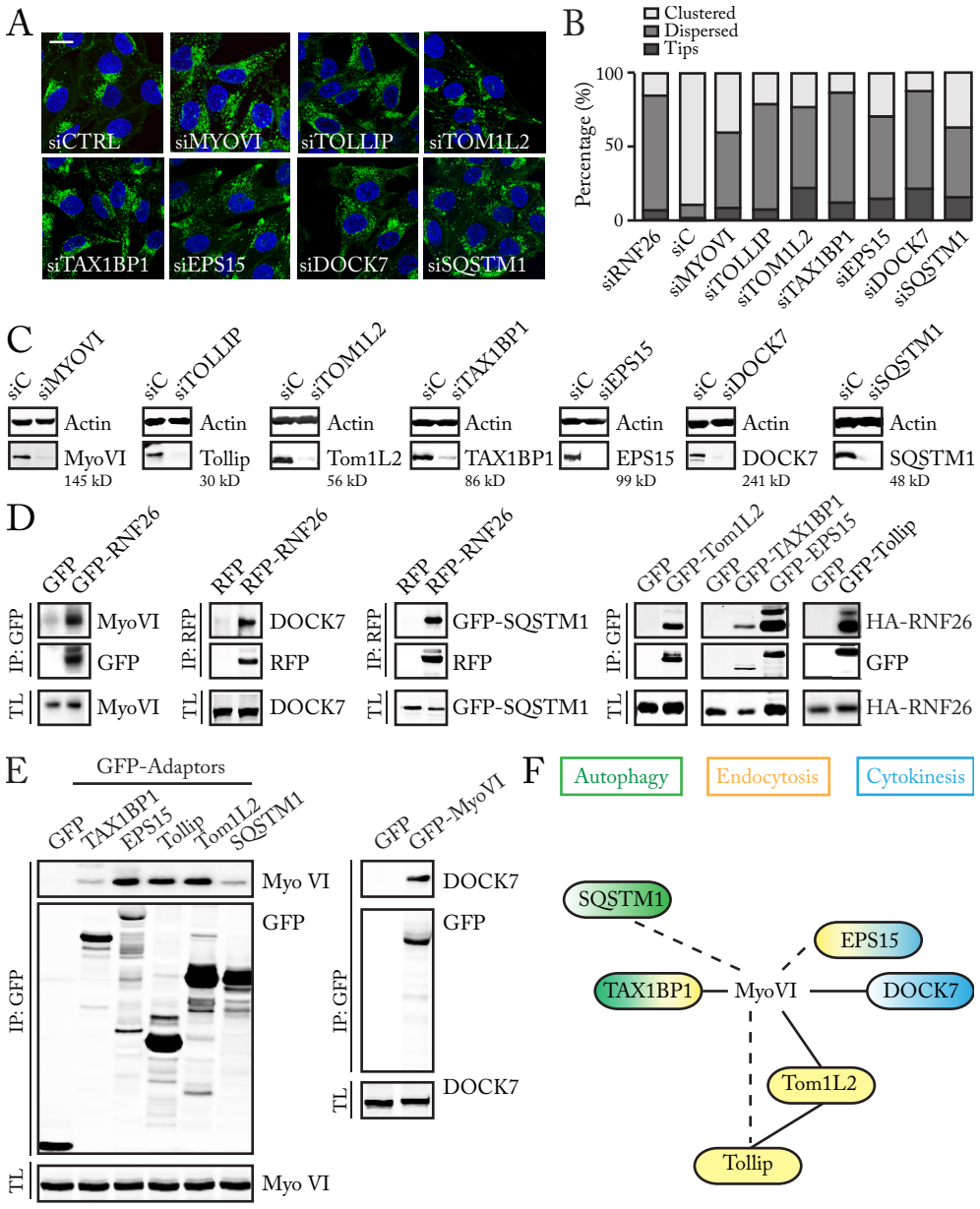


Figure 3 | **Identification of RNF26 interacting proteins.** (A) MelJuSo cells depleted for Myosin VI, Tollip, Tom1L2, TAX1BP1, EPS15, DOCK7 and SQSTM1 show dispersion of MHC class II (HLA-DR) containing vesicles (green) compared to control cells. The nucleus is stained by Hoechst (blue). (B) Quantification of the dispersion phenotype after depletion of RNF26 interacting proteins. (C) Depletion of the different RNF26 interacting proteins was visualized by western blot using antibodies recognizing endogenous proteins. Actin was used as a loading control. Protein levels of all proteins were strongly reduced after siRNA transfection. Molecular weight standard is indicated. (D) Co-immunoprecipitation of RNF26 and the by pull down identified interacting proteins. Immunoblots were probed with antibodies recognizing the different interacting proteins and RNF26. Interaction of

Figure 3 | **Continued**
Myosin VI, Tollip, Tom1L2, TAX1BP1, EPS15, DOCK7 and SQSTM1 with RNF26 was confirmed. (E) (left) Co-immunoprecipitation of Myosin VI with TAX1BP1, EPS15, Tollip, Tom1L2 and SQSTM1. Immunoblot was probed with antibodies recognizing endogenous Myosin VI and the GFP-tagged proteins. TAX1BP1, EPS15, Tollip, Tom1L2 and SQSTM1 all show a strong interaction with Myosin VI. (right) Co-immunoprecipitation showing an interaction between GFP-Myosin VI and endogenous DOCK7. Immunoblot was probed with antibodies recognizing DOCK7 and GFP-Myosin VI. (F) Based on published literature we placed Myosin VI in the middle of a protein network containing proteins known to play a role in autophagy (SQSTM1 and TAX1BP1), endocytosis (TAX1BP1, Tollip, Tom1L2 and EPS15) and cytokinesis (EPS15 and DOCK7). (Bar = 10μm)

ting (Figure 3C). The interaction between the candidates and full length RNF26 was further confirmed by Co-IP of ectopically expressed or endogenous proteins (Figure 3D). Remarkably, three of these candidates, namely TAX1BP1 [16], DOCK7 [17] and Tom1L2 [15], were already published to interact with Myosin VI. Since Myosin VI can interacts with many different proteins, we determined whether the other three candidates also interact with Myosin VI. Indeed, Tollip, EPS15 and SQSTM1 as well as the already published interactors Tom1L2, DOCK7 and TAX1BP1 interacted with Myosin VI in Co-IP experiments suggesting a central role for Myosin VI in RNF26 controlled endosomal positioning (Figure 3E). We then applied literature to place the various RNF26 interactors in networks in order to provide direction to the cell biology of this system. The various adaptor proteins could be place in three partially overlapping categories; autophagy (SQSTM1 [19] and TAX1BP1 [13]), endocytosis (EPS15 [20], Tom1L2 [21], Tollip [21,22] and TAX1BP1 [23]) and cytokinesis (EPS15 [24] and DOCK7 [17]) (Figure 3F). Additionally, Tollip has been shown to interact with Tom1L2 via its C-terminal Tom-binding Domain [21], suggesting that complex formation between RNF26 and Myosin VI may require binding of more than one of these adaptor proteins simultaneously. We identified various proteins interacting with the cytosolic RNF26 tail. These fall in overlapping networks that may control the actin-based motor protein Myosin VI. Interactions with the actin cytoskeleton could serve to preserve the intracellular organization of the endosomal system.

*Most identified adaptor proteins require ubiquitin-binding domains to interact with RNF26*
Domain structure analysis of the adaptor proteins identified by RNF26 pulldown, revealed that five out of six contain domains known to bind non-covalently to ubiquitin [25]. EPS15 contains a UIM and DUIM domain; Tollip a CUE domain; Tom1L2 a GAT domain and a VHS domain (Mizuno, 2003, Mol Biol Cell); TAX1BP1 contains two UBZ domains and SQSTM1 has a UBA domain. Only DOCK7 did not contain a ubiquitin-binding domain (Figure 4A). We mutated the ubiquitin interacting domain from the various proteins to evaluate the effect of ubiquitin binding on their interaction with RNF26. Four of the adaptors (TAX1BP1, Tom1L2, EPS15 and Tollip) interact only with RNF26 when they contain an intact ubiquitin interacting domain (Figure 4B-E). Ubiquitin binding was not required for the interaction between RNF26 and SQSTM1 (Figure 4F). SQSTM1 binds RNF26 in a ubiquitin-independent way, which is also the case for DOCK7 which binds RNF26 without the presence of a ubiquitin-binding domain (Figure 3D). As a result, the six RNF26 interacting proteins could be subdivided into two groups: scaffolding proteins (SQSTM1 and DOCK7), which bind RNF26 in a ubiquitin-independent way, and adaptor proteins (TAX1BP, Tollip, Tom1L2 and EPS15), binding ubiquitin dependent.

*RNF26 regulated ubiquitination of SQSTM1 and DOCK7 is important for their interaction*

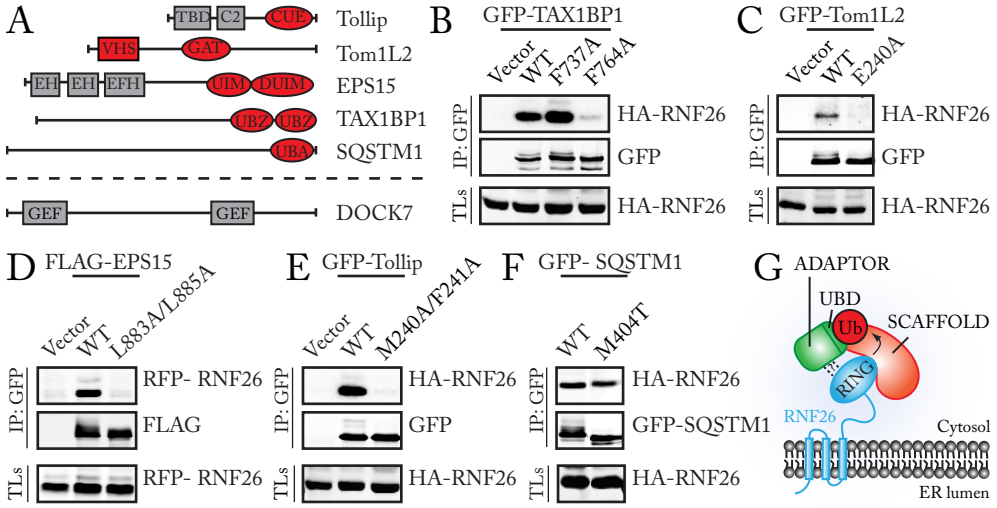


Figure 4 | **Most adaptor proteins require ubiquitin-binding domains to interact with RNF26.** (A) Representation of the different domains present in the identified RNF26 interacting proteins involved in endosomal positioning. Five out of 6 contain ubiquitin-binding domains. EPS15 contains a UIM and DUIM domain; Tollip a CUE domain; Tom1L2 a GAT and VHS domain; TAX1BP1 has two UBZ domains; SQSTM1 contains an UBA domain. Only the GEF DOCK7 does not contain one of the currently known ubiquitin-binding domains. (B-E) Mutations in the ubiquitin binding-domains of TAX1BP1 (F764A), Tom1L2 (E240A), EPS15 (L883A/L885A) and Tollip (M240A/F241A) show loss of binding to RNF26 in co-immunoprecipitation assays. (F) A mutation in the SQSTM1 domain known to interfere with ubiquitin binding (M404T) does not influence SQSTM1 binding to RNF26 in a co-immunoprecipitation assay. (G) Model showing two types of RNF26 interactors: scaffolding proteins (DOCK7 and SQSTM1) who interact with RNF26 independently of ubiquitin and adaptor proteins (TAX1BP1, EPS15, Tollip and Tom1L2) who depend on ubiquitin binding via their ubiquitin-binding domain to allow their interaction with RNF26.

*with the adaptor proteins*

Since Co-IP experiments show that adaptor proteins bind mainly non-ubiquitinated RNF26 (Figure 3D and Figure 4B-E), we surmised that adaptor proteins bind RNF26 with help of (currently unknown) ubiquitinated scaffolding proteins (Figure 4G). Scaffolding protein candidates are the ubiquitin-independent RNF26 binders SQSTM1 and DOCK7. To determine whether SQSTM1 and DOCK7 ubiquitination is affected by RNF26 we performed an ubiquitination-assay studying HA-SQSTM1 or endogenous DOCK7 in combination with either empty vector, RFP-RNF26 or (inactive) RFP-RNF26 C401S. Combined expression of HA-SQSTM1 and RFP-RNF26 resulted in many bands representing modified SQSTM1. Additionally, SQSTM1 was heavily ubiquitinated only in combination with the active form of RNF26 (Figure 5A). Also endogenous DOCK7 showed an increased ubiquitination when active RNF26 was co-expressed (Figure 5B). This suggests that RNF26 indeed affects SQSTM1 and DOCK7 ubiquitination. To further demonstrate SQSTM1 ubiquitination by RNF26 we determined the localization of GFP-SQSTM1, HA-RNF26 or inactive HA-RNF26 I382R and endogenous ubiquitin by confocal microscopy. GFP-SQSTM1 showed co-localization with both HA-RNF26 and the inactive HA-RNF26 I382R, but ubiquitin was only detected at SQSTM1 positive spots in the presence of active RNF26 (Figure 5C). These results also show that SQSTM1 stays localized to RNF26 after its ubiquitination and does not diffuse to other

sites. This supports our hypothesis that adaptor proteins interact with RNF26 via ubiquitinated SQSTM1 (or DOCK7). RNF26 would then first ubiquitinate SQSTM1 or DOCK7 which would then recruit Myosin VI and the membrane receptorsTom1L2, Tollip, TAX1BP1 and/or EPS15. We tested this for SQSTM1 and Tollip. Tollip binding to SQSTM1 was affected when the ubiquitin-binding domain of Tollip was mutated. This deletion did not affect the interaction between Tollip and its known binding partner Tom1 (Figure 5D). This illustrates the importance of Ubiquitin binding in the interaction between Tollip and SQSTM1 but not Tom1. The ubiquitin-binding domain of Tollip is also responsible for Tollip binding to DOCK7 (Figure 5E). To again test where in a cell these interactions occur, we used confocal microscopy. While SQSTM1 did co-localize with both HA-RNF26 and HA-RNF26 I382R, GFP-Tollip was only recruit-

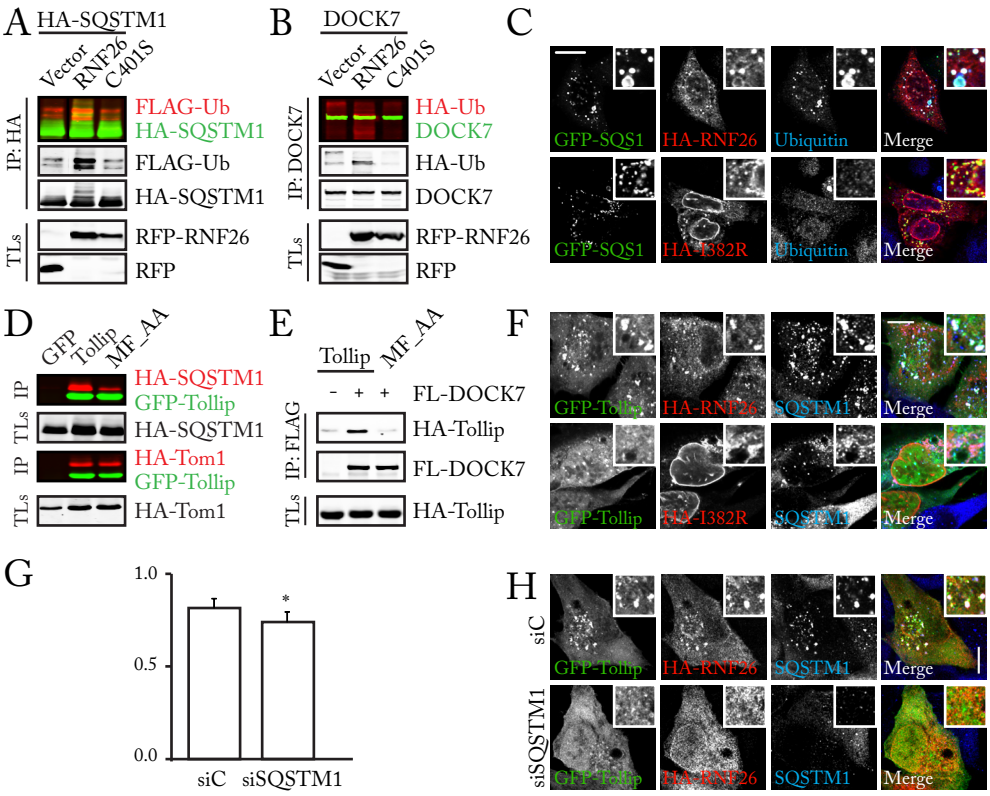


Figure 5 | **RNF26 regulated ubiquitination of SQSTM1 and DOCK7 is important for the recruitment of adaptor proteins.** (A) Ubiquitination-assay using HEK cells overexpressing FLAG-ubiquitin, HA-SQSTM1 and either RFP-RNF26, RFP-RNF26 C401S or empty vector shows increased ubiquitination of SQSTM1 in the presence of RNF26, but not the inactive mutant. (B) Ubiquitination-assay using HEK cells containing DOCK7 and overexpressing HA-ubiquitin in combination with either RFP-RNF26, RFP-RNF26 C401S or empty vector shows an increased ubiquitin signal after SQSTM1 immunoprecipitation in the presence of RNF26, but a reduced ubiquitin signal for the inactive mutant. (C) (upper panel) Cells overexpressing GFP-SQSTM1 (green) and HA-RNF26 (red) were fixed and stained for HA and endogenous ubiquitin (blue). RNF26, SQSTM1 and ubiquitin co-localize at bright spots at the ER membrane (white). (bottom panel) Cells overexpressing GFP-SQSTM1 (green), HA-RNF26 I382R (red) were fixed and stained for HA and endogenous ubiquitin (blue). RNF26 I382R and SQSTM1

Figure 5 | **Continued**
still co-localize (yellow), but ubiquitin is absent from these structures if RNF26 is inactive. (D) Co-immunoprecipitation of GFP-Tollip, GFP-Tollip mutant (MF_AA) and empty vector (green) with either HA-SQSTM1 or HA-TOM1 (red). Tollip and its ubiquitin-binding mutant bind equally well to Tom1, while binding of the ubiquitin-binding mutant of Tollip to SQSTM1 is reduced compared to wild type Tollip. (E) Co-immunoprecipitation of HA-Tollip or HA-Tollip mutant (MF_AA) with FLAG-DOCK7 shows reduced binding between DOCK7 and the Tollip ubiquitin-binding mutant compared to wild type Tollip. (F) (upper panel) Cells overexpressing GFP-Tollip (green) and HA-RNF26 (red) were fixed and stained for HA and endogenous SQSTM1 (blue). RNF26, SQSTM1 and Tollip co-localize at bright spots (white). (bottom panel) Cells overexpressing GFP-Tollip (green) and HA-RNF26 I382R (red) were fixed and stained for HA and endogenous ubiquitin (blue). RNF26 I382R and SQSTM1 still partially co-localize, but Tollip is completely absent from these structures if RNF26 is inactive. (G) Pierson's correlation coefficients of co-localization between GFP-Tollip and HA-RNF26 in control cells or cells depleted for SQSTM1. Co-localization between the two proteins is slightly but significantly reduced in SQSTM1 depleted cells. (H) Cells overexpressing GFP-Tollip (green) and HA-RNF26 (red) were fixed and stained for HA and endogenous SQSTM1 (blue). While control cells show clear co-localization between all three proteins, this is lost in cells depleted for SQSTM1. Both GFP-Tollip and HA-RNF26 show a more dispersed localization in the cytosol or ER membrane respectively if SQSTM1 is absent. Bar = 10μm, *$p<0.003$

ed when active RNF26 was present to (probably) ubiquitinate SQSTM1 (Figure 5F). To further illustrate that SQSTM1 is important in the interaction between RNF26 and Tollip, we studied the interaction between the two proteins in cells silenced for SQSTM1. Confocal images show a reduction in co-localization between HA-RNF26 and GFP-Tollip after SQSTM1 depletion (Figure 5H). Co-localization between RNF26 and Tollip was quantified by Pierson's correlation coefficients (Figure 5G). These experiments suggest that RNF26 ubiquitinates SQSTM1 and DOCK7 followed by recruitment of (one of) the endosomal adapter proteins like Tollip. These important (first) interactions between members of the endosomal-positioning complex appear to occur in ER microdomains.

*RNF26 Ubiquitinated adaptors interact with Myosin VI*

Binding of the adaptor protein to the ubiquitinated scaffolding protein will bring it in close proximity to RNF26. To determine if the recruited adaptor protein itself gets ubiquitinated by RNF26, we performed ubiquitination-assays on the different adaptors in the presence of over-expressed RNF26 or the inactive RNF26 mutant C401S. Indeed ubiquitination of GFP-TAX1BP1 and GFP-EPS15 was strongly increased by RNF26, but not by the inactive RNF26 mutant (Figure 6A). GFP-Tollip ubiquitination was increased after over-expression of both RNF26 or the RNF26 active Tail, and decreased by over-expressing the inactive mutant RNF26 C401S (Figure 6B).This indicates that the endosomal-positioning complex recruited by RNF26 becomes highly ubiquitinated.

How then is the Myosin VI motor recruited to the formed complex and is therea role for ubiquitin? Myosin VI also contains an ubiquitin-binding domain, called MIU (aa998-1031) [26] (Figure 6E). We again performed Co-IP experiments to test whether ubiquitin is involved in the interaction between the adaptor protein Tollip and Myosin VI. While wild type Tollip interacted with GFP-Myosin VI, no such interaction was detected between GFP-Myosin VI and the ubiquitin-binding domain mutant of Tollip (MF_AA) (Figure 6B,C). The ubiquitin-binding domain is also essential for efficient Tollip ubiquitination by RNF26, potentially since the ubiquitin-binding domain brings Tollip close to RNF26 (Figure 6B). To dissect between direct and indirect effects of RNF26 mediated ubiquitination of Tollip, we constructed Lysine-less Tollip mutants (we chose to mutate the four Lysine residues conserved between human and mice, namely K96, K162, K235 and

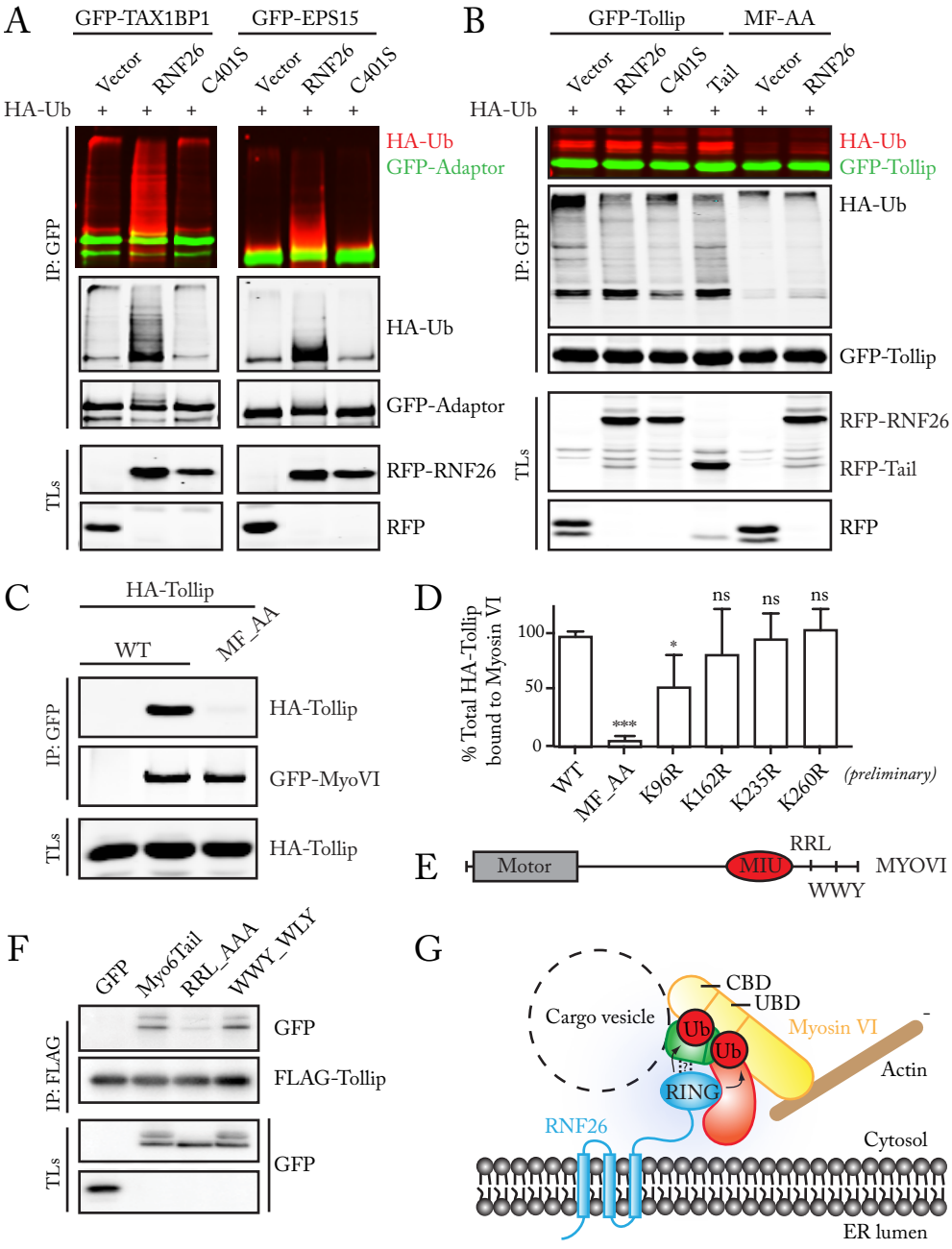


Figure 6 | **RNF26 mediated ubiquitination recruits the actin-based motor Myosin VI.** (A) Ubiquitination-assays using HEK cells overexpressing HA-ubiquitin, GFP-TAX1BP1 or GFP-EPS15 and either RFP-RNF26, RFP-RNF26 C401S or empty vector show increased ubiquitination of both TAX1BP1 and EPS15 in the presence of RNF26, in the presence of inactive RNF26 C401S a small reduction in ubiquitin signal can be observed. B. Ubquitination of GFP-Tollip and GFP-Tollip mutant (MF_AA) by several RFP-tagged RNF26 proteins was tested in a ubiquitin assay using HA-ubiquitin. Overexpression of RNF26 combined with GFP-Tollip shows an increase in the

Figure 6 | **Continued**
ubiquitin signal while the inactive RNF26 mutant C401S results in a decrease. Overexpression of only the Tail domain of RNF26 (containg the RING domain) shows a ubiquitin signal comparable to full length RNF26. The ubiquitin signal on GFP-Tollip mutant (MF_AA) is strongly reduced and almost absent, suggesting that the ubiquitin-binding mutant of Tollip is not or almost not ubiquitinated. (C) Co-immunoprecipitation experiment shows the importance of Tollip ubiquitination (or its binding to ubiquitin) for its interaction with the motor protein Myosin VI. Tollip mutant (MF_AA), which is not ubiquitinated and does not bind ubiquitin does not bind GFP-Myosin VI while wild type Tollip does. (D) Four Lysine(K)-mutants of Tollip and Tollip mutant MF_AA were tested for their ability to interact with GFP-Myosin VI in a co-immunoprecipitation experiment. Band were quantified and the percentage of total Tollip levels interacting with Myosin VI was calculated. Only the K96R mutation shows a significant decrease in Tollip binding to Myosin VI. Tollip mutant MF_AA does show an almost complete loss of Myosin VI binding. (E) Schematic representation of conserved domains present in Myosin VI. Myosin VI consists of a N-terminal motor domain and a C-terminal cargo-binding tail. The cargo-binding tail contains a MIU domain, which binds ubiquitin, and two protein binding 'hot-spots' RRL and WWY. (F) Co-immunoprecipitation experiment of FLAG-Tollip with either GFP-Myosin VI Tail or the two Myosin VI tail domain mutants (RRL to AAA and WWY to WLY) shows a role for the RRL motif in the interaction between Tollip and Myosin VI. (G) Model representing the mechanism behind RNF26 controlled Myosin VI-mediated endosomal localization. RNF26 is localized in the ER membrane where it recruits the scaffolding proteins SQSTM1 and/or DOCK7. This results in SQSTM1 and DOCK7 ubiquitination which recruits one or more adaptor proteins (Tollip, Tom1L2, EPS15 and TAX1BP1) connected to an endocytic vesicle. Myosin VI binds in a ubiquitin dependent way to the whole complex initiating tethering (or short distance movement) of the vesicle to the actin network. $^{*}p<0.01$, $^{***}p<0.0001$

K260, into Arginine (R)) and tested their interaction with Myosin VI in a Co-IP experiment. Only the K96R mutation slightly affected binding between Tollip and Myosin VI, but not nearly as much as the ubiquitin-binding mutant of Tollip (MF_AA) (Figure 6D). This shows that mutation of one single Lysin is not enough to prevent Myosin VI binding to Tollip and suggests that multiple ubiquitins, or additional domains (or proteins) are involved. Which other domains could be involved in binding? Besides the Myosin VI UIM domain, the Myosin VI tail contains two other binding sites (RRL (aa 1084-1086) and WWY (aa 1160-1162)) reported to be important in the interaction with Myosin VI adaptor proteins [11]. These binding 'hot-spots' were mutated and tested for interactions with Tollip by Co-IP experiments. The RRL binding site on Myosin VI was identified as the binding site for Tollip (Figure 6F). This binding is likely stabilized by the additional binding of Myosin VI to ubiquitin. Based on our data, we build a model on the mechanism of RNF26 regulated Myosin VI-mediated endosomal positioning (Figure 6G). RNF26 localizes in the ER membrane and their recruits and ubiquitinates the scaffolding proteins SQSTM1 and DOCK7. The adaptor proteins Tollip, EPS15, Tom1L2 and TAX1BP1, bound to different types of endosomal vesicles, bind to the ubiquitinated scaffolding protein via their ubiquitin-binding domains bringing them in close proximity of RNF26 leading to their ubiquitination. Myosin VI is recruited to the highly ubiquitinated complex via its MIU and protein binding domains. Myosin VI interacts with actin, thereby tethering the various endosomes in the correct position. Additionally, the scaffolding protein DOCK7 contains GEF activity for the small GTPases Rac1 and cdc42 that may help in local actin polymerization onto which the Myosin VI motor docks to remain the positioning of endosomes.

*RNF26 controlled endosomal vesicle localization is involved in mitosis.*

Why do cells have such a unique intracellular distribution of endosomal organelles? And what would happen if this distribution would not exist and endosomes would be randomly dispersed? A highly important biological process requiring endosomal dispersion is cell division. Cells have to lose their normal

endosomal organization when they prepare for mitosis to allow an equal share for both daughter cells. This may involve the RNF26 controlled endosomal positioning system. To show endosomal dispersion during mitosis we imaged mCherry-CD63 labeled endosomes during one round of cellular division. Still images show that endosomes indeed disperse during metaphase, and anaphase and cluster again at the beginning of cytokinesis (Figure 7A). To determine if RNF26 depletion affects mitosis, we then measured the time a cells needs to go through the different steps of mitosis in either RNF26 containing cells (siCTRL) or RNF26 depleted cells (siRNF26). RNF26 containing cells need around 90min between start and finish of one round of cellular mitosis. This was markedly increased after RNF26 depletion. A full round of mitosis then required around 160min (Figure 7B). This delay mainly concentrated at the end of mitosis, especially at the process of daughter cell separation, cytokinesis, which is in line with the reported role of Myosin VI in cytokinesis (Figure S4A and B) [14]. Published data obtained from Myosin VI depleted cells show 14% multinucleated cells of the total population, which indicates that cells failed to undergo successful cytokinesis in the absence of Myosin VI [14]. To determine if RNF26 is like myosin VI important in cytokinesis, we determined the percentage of multinucleated cells after RNF26 depletion. We found 6.6% of RNF26 depleted cells showing a multinucleated phenotype comparable to 1% of control transfected cells (Figure 7C and D). Of note, multinucleated cells usually die and the real number of cell failing in cytokinesis when RNF26 is silenced may be considerably higher. The importance of RNF26 during mitosis was also visualized by confocal microscopy. MelJuSo cells depleted for RNF26 and control treated cells were fixed, stained for LEs (MHC class II) and REs (TfR), and imaged at different stages of the cell cycle. While RNF26 depletion does not affect endosomal localization during metaphase and anaphase, when endosomes disperse, RNF26 depletion did show dispersion of endosomes during cytokinesis (Figure 7F), while endosomes cluster again in control cells (Figure 7E). Control cells show two clusters of endosomes, one surrounding its MTOC, the other directed towards the intracellular bridge. The latter cluster may function in the delivery of membranes and the abscission machinery towards the midbody. This transport is thought to be Myosin VI mediated. The localization of Myosin VI in mitotic cells has been studied recently. Myosin VI is known to localize to the spindle pole in prophase, at the walls of the ingression furrow during anaphase and close to the midbody in the intracellular bridge during cytokinesis [14]. We expect changes in Myosin VI localization in RNF26 depleted mitotic cells (in progress). These experiments suggest a role for RNF26 in the control of the last step of mitosis, cytokinesis.



**Discussion**

The intracellular location of organelles is well defined in most cells. Like organelles, also the endosomal compartments, like the TGN, early endosomes, and late endosomes/lysosomes all have a organized non-random cellular distribution. Although this is observed for over five decades, the molecular mechanism behind the organized distribution of different endocytic compartments is still unclear. Here we decipher the molecular mechanism controlling the intracellular distribution of the entire endosomal pathway. We show that it is under control of the ER localized multipass transmembrane E3 ligase RNF26. This protein interacts in a ubiquitin independent way with two proteins, SQSTM1 and DOCK7. These proteins act as a scaffold for other proteins that specify the targeting to the various endocytic structures; TAX1PB1 for the TGN, EPS15 for early and Tollip/Tom1L2 for late endosomes. Members of

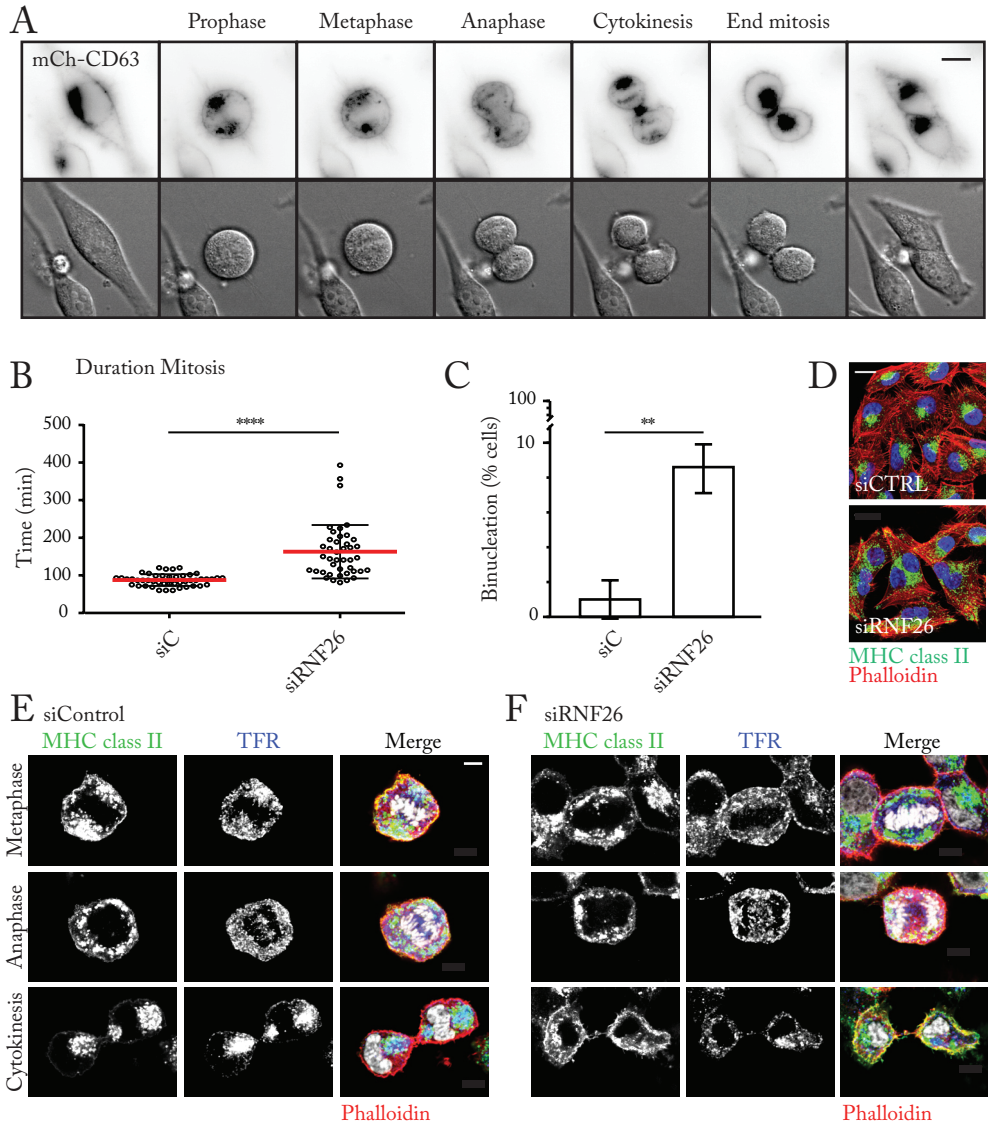


Figure 7 | **RNF26 regulated endosomal localization plays a role in mitosis.** (A) MelJuSo cells stably transfected with mCherry-CD63 (late endosomes) were imaged during one round of the cell cycle. Upper panel shows mCherry-CD63; the bottom panel the transmitted light images. Late endosomes disperse during the early phases of mitosis but re-cluster when cytokinesis occurs. (B) RNF26 depleted cells and cells treated with a non-targeting siRNA were followed during their cell cycles. Time between the onset of mitosis (when the cell rounds up) and the end of mitosis (when the two daughter cells are separated) was determined for both conditions. RNF26 depleted cells show a prolonged duration of mitosis. On average RNF26 depleted cells spend 160min in mitosis, while control treated cells had a mitotic cycle of only 90min. (C,D). The percentage of bi-nucleated cells was determined in cells depleted for RNF26 and control siRNA treated cells. After three days of silencing, the cells were fixed and stained for MHC class II (late endosomes), phalloidin (actin cytoskeleton) and Hoechst (nucleus). The amount of bi-nucleated cells was determined by eye. Around 9% of RNF26 depleted cells were bi-nucleated whereas bi-nucleation in the control sample was quite rare, only 1%. Confocal images show bi-nucleation in RNF26 depleted fixed cells. (E) Control cells were fixed and stained for MHC class II, TfR, actin (Phalloidin) and the nucleus. Images of cells in different

Figure 7 | **Continued**
stages of the cell cycle show endosomal dispersion during prophase and metaphase, while endosomes cluster again during cytokinesis forming two clusters of endosomes on opposite sides of the nucleus. (F) RNF26 depleted cells were fixed and stained for MHC class II, TfR, actin (Phalloidin) and the nucleus. Images of RNF26 depleted cells in different stages of the cell cycle show, like control cells, endosomal dispersion during prophase and metaphase, but endosomes are still dispersed during cytokinesis. Bar = 10μm, ****p<0.0001, **p<0.001

the formed complex are ubiquitinated by the ER localized RNF26 and recruit Myosin VI connected to actin. The ER thus controls the positioning of the entire endocytic pathway by controlling the recruitment of the motor protein Myosin VI. The scaffold DOCK7 has GEF activity for the small GTPases Rac1 and Cdc42 [27] which usually initiates polymerization of actin which is required for the activity of myosin motors. It is tempting to speculate that DOCK7 GEF activity prepares local cytoskeletal networks allowing the tethering of endosomal vesicles by Myosin VI and their positioning inside the cell.

Why needs a cell a mechanism to control the positioning of endosomes? A likely cellular process requiring a mechanism controlling endosomal localization is mitosis. First, during cell division, organized endosomal positioning should be lost to allow random endosome dispersion ensuring equal sharing of the compartments between the two daughter cells [28]. Second, it is assumed that during the last step of mitosis (cytokinesis) when the two daughter cells are separated additional membranes are required so seal the 'wound' [29]. These membranes have been proposed to be derived from the Golgi as secretory vesicles or from early endosomes [30] although in fact late endosomal multivesicular bodies contain most membranes per unit. Our data suggest that loss of correct positioning of endosomes indeed delays cytokinesis. We show that cytokinesis often fails in RNF26 depleted cells, resulting in multinucleation (like published for Myosin VI [14]. The mechanism described here not only provides a potential mechanism of membrane delivery to the side of daughter cell separation, but also appears to control the timing of mitosis. Endosomes disperse at the early phases of mitosis, prophase and metaphase, but re-organize during anaphase and cytokinesis. Whether loss of controlled endosomal positioning is due to ER repositioning during mitosis (Chapter 3) leading to disruption of the RNF26 controlled endosomal-positioning complex, or inactivation of RNF26 ligase activity at this step in mitosis, is currently unknown. Yet, the unique dynamics of the various compartments that interact to exchange information on positioning and their dramatically altered positioning during mitosis are processes that are poorly understood. We here provide the first description of a pathway controlling the positioning of the endosomal pathway in cells.

***Below, more specific information on the various aspects of this new pathway is provided.***

*RNF26 is localized in the ER membrane:* The localization of RNF26, in the ER membrane, makes it a perfect regulator at different cellular locations. The ER spreads throughout the whole cell and has been shown to form contact sites with different vesicles and even organelles. At these contact sites two opposing membranes come in close proximity, but they do not fuse [4,5]. It would be interesting to determine whether RNF26 is localized at these contact sites since these sites are ideal locations for RNF26 to ubiquitinate its targets on endosomes.

*Identification of RNF26 interacting proteins involved in endosomal transport:* We identified 18 potential RNF26 interacting proteins by GST-pulldown and mass spectrometry.

These candidates were further selected for their role in endosomal transport by an siRNA-based screen. Silencing of 7 candidates resulted in a similar phenotype as observed by RNF26 depletion, namely dispersion of endosomes. This suggests a role for these proteins in RNF26 regulated endosomal positioning. But what about the other 11 proteins identified by mass spectrometry? These candidates may also be involved in endosomal positioning but this was not confirmed by the siRNA-based screen. There are multiple reasons for this. First, siRNAs never result in a 100% knock down, if there is still enough protein left to fulfill its function, no effect will be observed. Second, redundancy could make up for the loss of the silenced protein. Third, if the protein is stable, silencing for three days will still result in the presence of functional protein. Fourth, the proteins could be negative regulators of RNF26. A candidate for such a negative regulator of RNF26 is USP15, a de-ubiquitinating enzyme (see below). Another, more likely, option is that these other candidates interact with RNF26 to perform functions different from endosomal positioning. The fact that we indeed identify RNF26 interactors that are not involved in endosomal transport, suggests additional functions for RNF26.

Seven proteins were identified as RNF26 interacting proteins involved in endosomal transport, including the actin-based motor protein Myosin VI. Three other candidates (TAX1BP1, DOCK7 and Tom1L2) have already been described to interact with Myosin VI. TAX1BP1 was found to interact with Myosin VI via its two C-terminal Zink-Fingers at the TGN and vesicles in the perinuclear area, where it acts as negative regulator of secretion [16]. TAX1BP1 is also present on autophagosomes, where it recruits Myosin VI bound endosomes [13]. DOCK7, is a Guanine Exchange Factor for the GTPase Rac1 and Cdc42, that is involved in actin polymerization. Its interaction with Myosin VI suggests a function of this GEF in Myosin VI-dependent actin cytoskeleton regulation [17]. Tom1L2 is a close homologue of Tom1 and binds Myosin VI via its IEVWL motif at its C-terminus [23]. Tom1L2 has been found on endosomes [21] and on the Golgi after overexpression [31]. Interestingly, we also identified the Tom1L2 interacting protein Tollip [21]. Tollip has been shown to localize to endosomal membranes (containing PI(3)P and PI(4,5)P2) via its C2-domain [32] recruiting Tom1L2 and ubiquitinated proteins to endosomes. Its interaction with Tom1L2 makes Tollip a likely candidate to interact (either direct or indirect) with Myosin VI. Indeed Tollip, as well as the two remaining candidates EPS15 (involved in clathrin mediated endocytosis) and SQSTM1 (targeting ubiquitinated proteins to autophagosomes [19], were found to interact with Myosin VI in a Co-IP experiment. It is interesting to note that the Myosin VI and RNF26 interactors are known to localize to different subsets of endosomes. These include TAX1BP1 (Trans Golgi Network and autophagosomes), DOCK7 (unknown), Tom1L2 (Early and late endosomes), Tollip (Early and Late endosomes), EPS15 (Clathrin-coated vesicles and at the Trans Golgi Network [33]) and SQSTM1 (autophagosome). The presence of the adaptor proteins on different types of vesicles makes it a likely possibility that Myosin VI interacts with the different adaptors on different subsets of endosomes regulating their localization via a similar mechanism involving RNF26 regulated ubiquitination events.

*Interactions within the protein complex:* A large multi-protein endosomal-positioning complex is formed after targeted ubiquitination by the E3 ligase RNF26, resulting in interactions between various ubiquitin-binding domain containing adaptors, scaffolding proteins and Myosin VI. While RNF26 is

involved in the ubiquitination of the different proteins, the ubiquitin-binding domains (and possibly other unknown interacting motifs) hold the complex together. Many different ubiquitin-binding domains exist, all having unique abilities and perhaps specificities to interact with ubiquitin [34] but in general the ubiquitin-binding domains have low affinity for mono-ubiquitin resulting in a weak interaction. The presence of different ubiquitin-binding domains in almost all proteins being part of the identified endosomal-positioning complex will transform all (individually) relatively weak interactions with ubiquitin into a stable complex. Additionally, some of the ubiquitin-binding domains have properties which strengthen their interaction with ubiquitin. For example, some ubiquitin-binding domains can interact simultaneously to two ubiquitin moieties, like the GAT domain in Tom1L2 [35] and the DUIM domain present in EPS15 [36]. Furthermore, the interacting protein can contains multiple ubiquitin-binding domains recognizing multiple ubiquitin moieties. This is a likely option for EPS15 (has one UIM followed by a DUIM domain), and TAX1BP1 (containing two UBZ domains). Besides ubiquitin-based interactions, the endosomal-positioning complex is further stabilized by interactions between the adaptor proteins and Myosin VI. Two interaction hotspots, namely RRL (aa 1084-1086) and WWY (aa 1160-1162), have been identified at the C-terminal cargo binding tail of Myosin VI. Tollip (Figure 6C), EPS15 (data not shown) and TAX1BP1 [13,16] can interact with the RRL motif. The interaction sites for DOCK7, Tom1L2 and SQSTM1 still have to be determined. The Myosin VI interaction hotspots contain only 3aa for protein binding, which points towards a weak interaction, explaining why Myosin VI regulated transport is likely stabilized by a complex of multiple proteins.

Recent preliminary results gave us better insight into the binding mechanism of the scaffolding proteins SQSTM1 and DOCK7 to RNF26. Confocal microscopy analysis of cells overexpressing both RNF26 and SQSTM1 show co-localization between these proteins on clustered 'dots' in the ER membrane (Figure 5C), while in SQSTM1 depleted cells RNF26 is localized randomly in the ER membrane (Figure 5H) This shows that RNF26 and SQSTM1 molecules cluster at specific areas of the ER. Of note, these clusters also contain Tollip (Figure 5F). Both SQSTM1 and DOCK7 bind to RNF26 independently of ubiquitin, but there are also differences in RNF26 binding between the two proteins. This became clear by co-immunoprecipitation experiments used to determine the interaction of either SQSTM1 or DOCK7 with RNF26 mutants or only the Tail fragment of RNF26 (Figure 8A). SQSTM1 does not bind to the I382R and C401S mutants of RNF26. Since both mutants lose their ability to bind to E2 enzymes, this suggests that SQSTM1 needs the E2 to form a stable interaction with RNF26. In contrast, DOCK7 still interacts with the I382R mutant of RNF26 but not the C401S mutant (we expect that the C401S mutation leads to a bigger conformational change than the I382R mutation explaining the lost interaction). That binding of DOCK7 occurs independently of the E2 is further suggested by the incredible binding affinity of DOCK7 for the tail-domain of RNF26 (Figure 8A). Since DOCK7 binds weaker to full length RNF26 than the tail domain alone, the interaction between DOCK7 and the tail must be inhibited in reality. This inhibition could be due to restrictions in space; the ER membrane could be in the way, or DOCK7 cannot bind to the RNF26 tails that are to close together in the cluster since DOCK7 is a huge protein (250kD). Based on this data we build a highly preliminary model where SQSTM1 molecules bind to the clustered RNF26 molecules interacting with its E2

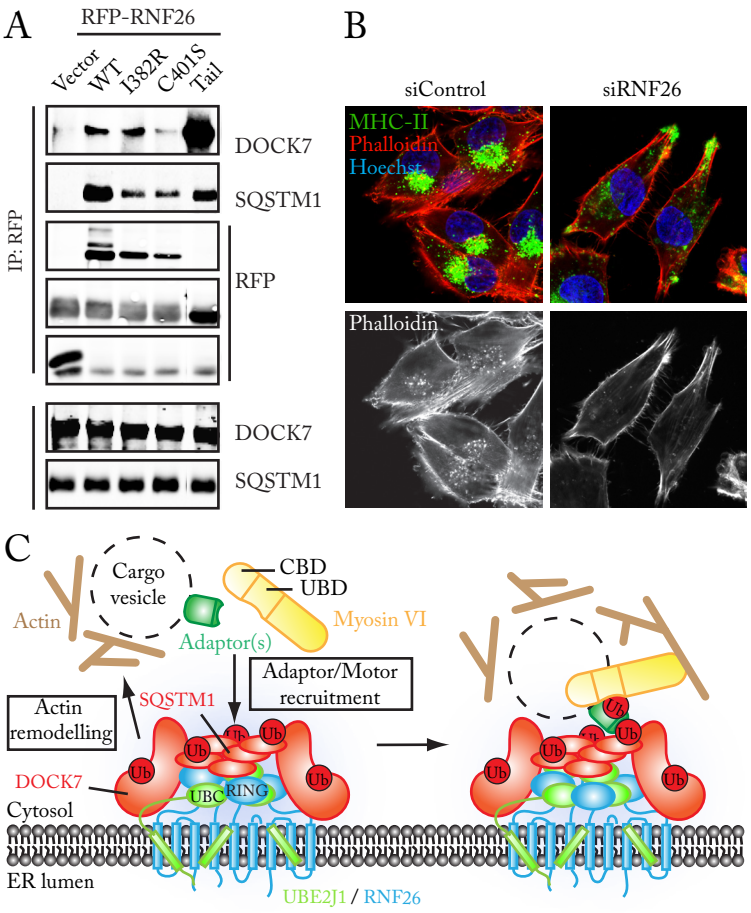


Figure 8 | **Hypothetical model: SQSTM1 and DOCK7 interact differently to RNF26.** (A) Co-immunoprecipitation experiments in cells overexpressing RFP-RNF26, RFP-RNF26 mutants (I283R and C401S), RFP-RNF26 Tail or empty vector show different interaction patterns for RNF26 with either endogenous SQSTM1 or DOCK7. SQSTM1 binds equally to wild type RNF26 and the Tail domain but its interaction with the two RNF26 mutants is strongly reduced. DOCK7 binds properly to wild type RNF26 and the RNF26 mutant I283R, while its interaction with the RNF26 mutant C401S is lost. DOCK7 binding to RNF26 is strongly increased after expression of the RNF26 Tail domain. (B) Control cells and cells depleted for RNF26 were fixed and stained for MHC class II (green), Transferrin Receptor (Blue) and actin (Phalloidin, Red/white). Control cells show the presence of actin-structures close to the cluster of endosomes at the perinuclear area, while these actin structures are absent in RNF26 depleted cells. (C) Hypothetical model showing a cluster of RNF26 E3 ligases and their E2 enzymes localized in the ER membrane. SQSTM1 is recruited to this cluster of RNF26 molecules and becomes ubiquitinated. The presence of ubiquitin leads to the recruitment of adaptor proteins bound to endosomes and to the recruitment of the motor protein Myosin VI. DOCK7 is recruited to the more spacial binding sites at the sides of the complex and becomes ubiquitinated. GEF activity of DOCK7 leads to actin remodeling providing actin filaments for the Myosin VI motor. Myosin VI interacts with the actin-filaments leading to proper endosomal localization. Bar = 10μm

enzyme, while DOCK7 binds to the RNF26 molecules at the boundaries of the cluster where is has enough space to bind RNF26 and to perform its function in actin-remodeling. This led to a model with two 'arms': one contains DOCK7 binding to RNF26 leading

to actin remodeling essential to keep Myosin VI and the vesicle on its proper place, while SQSTM1 leads to the recruitment of adaptors, the endosomal vesicle and Myosin VI. This recruitment leads to RNF26 mediated ubiquitination stabilizing the whole complex (Figure 8C). A role for DOCK7 in actin remodeling after recruitment by RNF26 was visualized by confocal microscopy. Phalloidin staining (actin) in control cells shows the presence of actin in close proximity to the clustered endosomes, whereas this is absent in RNF26 depleted cells (Figure 8B).

*Identification of an E2 enzyme for RNF26:* Formation of the endosomal-positioning complex, and thus Myosin VI mediated endosomal positioning, depends on RNF26 E3-ligase activity. RNF26 contains a RING domain, which requires an E2-enzyme to be able to ubiquitinate target proteins. To identify the E2 of RNF26, we performed an siRNA-based E2 enzyme screen. As a read-out we determined endosome localization by confocal microscopy and determined which E2 enzymes are involved in endosomal positioning showing a similar phenotype to RNF26 after their depletion (these results are described in Chapter 5). The screen revealed several candidates under which the ER membrane localized E2 enzyme UBE2J1, which will be described in more detail in chapter 5 [37]. The fact that we did not find an E2 in our protein pull-down experiments may be due to the use of the tail domain of RNF26 as bait to identify interaction partners. We may have missed proteins binding to the transmembrane domains of RNF26, which may be the case for the E2 enzyme UBE2J1. Potentially the single TM domain of UBE2J1 enters the 4 TM domains of RNF26 to stabilize the E2:E3 interaction. This is currently tested.

*Monomer or Dimer?* Although many studies have been devoted to answer the question if Myosin VI acts as a dimer or a monomer, the answer is not set yet. Originally, Myosin VI was expected to function as a dimer, since the Myosin VI tail domain contains a repeating sequence predicted to form a coiled-coiled α-helical involved in dimerization [38]. Nevertheless, the endogenous pool of Myosin VI has been shown to be almost completely monomeric (<1% dimeric) [39]. Also FRAP studies have shown that Myosin VI likely functions as a monomer, or in a dynamic equilibrium between monomer/dimer [40]. Transient dimerization of Myosin VI may be induced after binding to its cargo [11,41-43]. A candidate to selectively dimerize MyosinVI is the adaptor protein Tollip. Tollip contains a CUE domain at its C-terminus, which is not only known for its ability to bind ubiquitin, but also functions in Tollip dimerization [44]. Each of the two Tollip molecules can interact with Myosin VI bringing them together for temporal dimerization. Regulation of the monomeric/dimeric Myosin VI state may control its cellular functions like transporting or tethering.

*Transport or tethering?* Monomeric Myosin VI is expected to function as a non-processive motor with a step size of 18nm [39], while dimeric Myosin VI has the ability to moving processive with steps of 30-36nm [41]. As a result, monomeric Myosin VI may mainly function to anchor substrate to the actin network [45] whereas dimeric Myosin VI has a transporting function. Depletion of RNF26 and Myosin VI results in endosomal dispersion. Therefore we assume that RNF26 controls the interaction between Myosin VIand endosomes. Active RNF26 leads to a connection between Myosin VI and the endosomes resulting in their stabilized localization. Movement of the endosome only occurs following inactivation of the interaction between Myosin VI and the endosomes. Tethering of vesicles via monomeric Myosin VI is a likely option since it will keep the

vesicles on location (like shown for Myosin VI interacting with TAX1BP1 at the TGN [16]), but also transport could be involved by cargo-induced dimeric Myosin VI resulting in a continuous balance of transporting vesicles back and forward to their proper locations. Another option is tethering of vesicle via dimeric Myosin VI to the actin network, having each Myosin VI head interacting with another actin filament [46]. Furthermore Myosin VI has been shown to modulate the actin cytoskeleton together with DOCK7. Myosin VI regulated actin network may form a tight network around the vesicle to keep it in place, as shown for melanosomes [47]. Since each endosome has its own requirements according to its localization, RNF26 may couple Myosin VI to its specific interaction partners. The interaction partner decides the target compartment and tethering or transient short distance transport along actin. We propose that Myosin VI is responsible for correctly localized endosomes under steady state conditions. Inactivation of RNF26 by siRNA or -perhaps- during mitosis allows loss of positioning. How RNF26 is inactivated during mitosis, is as yet unclear.

*Myosin VI couples endocytosis to autophagy:* Autophagy is an essential cellular mechanism providing the cell with nutrients in case of starvation. It also clears the cell from unneeded or harmful materials, like damaged organelles and protein aggregates. Proteins targeted for autophagocytosis are often labeled by ubiquitin, which is recognized by ubiquitin-binding domain-containing proteins like TAX1BP1 and SQSTM1. TAX1BP1 and SQSTM1 contain LIR domains recruiting LC3 and leading to the formation of a double-membrane autophagosome [48]. The autophagosome will fuse with an endosome/lysosome followed by degradation of the destined proteins. Myosin VI has been shown to play a role in bringing together the autophagosome and the endosome/lysosome, via Tom1/Tom1L2 at the endosomal membrane and TAX1BP1 at the autophagosome [13]. We have shown that TAX1BP1, SQSTM1 and Tom1L2 are ubiquitinated by RNF26 leading to their interaction with Myosin VI, making RNF26 a potential regulator of autophagy in addition to regulating the positioning of the endosomal pathway (not further studied).

*RNF26 potentially regulates Myosin VI dependent endosomal transport during cytokinesis:* When we imaged endosomes during mitosis in MelJuSo cells we noticed that endosomes were dispersed during early phases of mitosis, but re-positioned during anaphase, forming a secondary cluster directed towards the interconnected bridge during cytokinesis. Myosin VI has already been suggested to play a role in transporting recycling endosomes towards the cleavage furrow and the intercellular bridge during anaphase and cytokinesis respectively [14,49]. We expect a role for RNF26 in the regulation of Myosin VI dependent endosomal transport during cytokinesis, since RNF26 depletion leads to multinucleation. The adaptor protein EPS15 has also been published to result in multinucleated cells after depletion [24], suggesting that it is also a potential adaptor protein candidate for Myosin VI regulated endosomal positioning during cytokinesis.

*USP15 may de-ubiquitinates proteins during mitosis:* The observed dispersion of endosomes during the first phases of mitosis suggests that RNF26 induced ubiquitination should be terminated during these phases. Ubiquitination can be reversed by de-ubiquitinating enzymes (DUBs), like USP15. USP15 was found in our mass spectrometry data as a potential interaction partner of RNF26. Possibly USP15 becomes active during the first stages of mitosis where after it de-ubiquitinates RNF26 targets resulting in inactivated Myosin VI regulated endo-

somal positioning and thus dispersion. Activation of USP15 may be regulated by phosphorylation, since some DUBs have already been shown to become phosphorylated in a cell cycle dependent manner [50].

*Conclusion:* Organized positioning of endosomes in the cell cytosol, instead of their random dispersion, has been observed for a long time. We provide here the first molecular mechanism responsible for proper endosomal positioning, controlled by the ER localized E3 ligase RNF26. We show how RNF26 first associates to scaffolding proteins leading to the recruitment of several endosomal membrane-bound adaptor proteins. Ubiquitination by RNF26 of the different proteins in the complex is required for complex formation and to recruit the Myosin VI motor. As a result, endosomal membranes find their characteristic position in cells. We show that proper control of endosomal positioning is critical for mitosis where this process is carefully timed.



**Material and Methods**

***Cell Lines:*** Wild type (wt) MelJuSo cells, human melanoma cell line were cultured in IMDM (Gibco) supplemented with 7.5% fetal calf serum (FCS, Greiner). Human HEK293T cells and HeLa cells were cultured in DMEM (Gibco) supplemented with 7.5% fetal calf serum (FCS, Greiner) and Penicillin/Streptomycin (Invitrogen).

***Antibodies:*** (Confocal Microscopy) Rabbit anti-human HLA-DR [51], mouse anti-TfR (Invitrogen 905963A), mouse anti-EEA1 (mAb 610457, BD transduction laboratories), mouse anti-CD63 NKI-C3 [52], sheep anti-TGN46 (A59AHP500, Bioconnect), rabbit anti-Giantin (Covance PRB-114C), mouse anti-Golgin-97 (CDF4, A21270, Invitrogen), mouse anti-ubiquitin (mAb, P4D1, sc-8017, Santa Cruz), anti-SQSTM1 (mAb, sc-28359, Santa Cruz), Rat anti-HA (3F10, Roche) and mouse anti-HA (mAb, HA.11 (16B12), Covance MMS-101R), were used to stain HLA-DR, EEA1 (Early endosomes), CD63 (Late endosomes), TGN46 (Trans Golgi Network), Giantin (Golgi), ubiquitin, SQSTM1 and HA-tagged proteins respectively, followed by secondary Alexa-dye coupled antibodies (Invitrogen) for detection by confocal microscopy. Hoechst (2 µg/ml, 33342, Invitrogen), MitoTracker red CMXRos (M7512, Invitrogen; 500nM added for 30min before fixation) and Phalloidin-Alexa568 (0.4 U/ml, Molecular Probes) were used to stain the nucleus, mitochondria and the actin network for detection by confocal microscopy. (Western Blotting) rabbit anti-DOCK7 (pAb, ab118790, Abcam), mouse anti-SQSTM1 (mAb, sc-28359, Santa Cruz), rabbit anti-MyosinVI (pAb, ABT42, Millipore) and rabbit anti-Myosin #3943 (gift from F. Buss), goat anti-Tollip (sc27315, Santa Cruz), rabbit anti-Tax1bp1 (A303-791A, Bethyl), rabbit anti-Tom1l2 (pAb, ab96320, Abcam), rabbit anti-Eps15 (pAb, sc-1840, Santa Cruz), rabbit anti-mGFP [3], mouse anti-HA (HA.11 (16B12), Covance MMS-101R), anti-HA-PO (Roche, 2013819001), anti-mRFP [3], rabbit anti-FLAG (F7425, Sigma), mouse anti-FLAG M2 (F3165, Sigma) and mouse anti B-actin (AC-15, Sigma) followed by secondary Rabbit anti-Mouse-PO (P0161, Dako) or HRP-Protein A (10-1023, Invitrogen) were used for detection of endogenous or overexpressed proteins on western blot. Secondary IRDye 800CW Goat anti-rabbit IgG (H+L) (926-32211, Li-COR), IRDye 800CW Goat anti-mouse IgG (H+L) (926-32210, Li-COR), IRDye 680LT Goat anti-rabbit IgG (H+L) (926-68021, Li-COR) and IRDye 680LT Goat anti-mouse IgG (H+L) (926-68020, Li-COR) were used for detection using the Odyssey Classic imager (Li-Cor). (Immunoprecipitation) Anti-mRFP [3], anti-mGFP [3], rabbit anti-FLAG (F7425, Sigma), anti-

HA (12CA5, gift from Dr. H. Ovaa, NKI, Amsterdam, NL) and anti-Dock7 (pAb, ab118790, Abcam) were used for immunoprecipitation of tagged or endogenous proteins. (Electron Microscopy) An antibody against human RNF26 was produced in rabbit after immunization with recombinant GST-RNF26 (aa 304-433) and used for detection of endogenous RNF26 by Electron Microscopy (the anti-RNF26 antibody was purified before use (see below)). Rabbit anti-PDI (H. Ploegh, MIT, Boston) was used as a ER marker for Electron Microscopy.

Anti-RNF26 antibody purification: Antigen (GST-RNF26 aa 304-433) was coupled to CNBr-activated sepharose 4B (GE healthcare) according to manufacturer's instructions. Briefly, dry resin was washed and swollen in 1mM HCl (250 ml/gram resin) before allowing it to react with antigen. Antigen dissolved in 0.1M sodiumbicarbonate was added to the bead slurry, such that the beads are covered in sufficient solvent. The final concentration of antigen on the beads was calculated as 1mg of antigen/ml of bead slurry. After overnight incubation at 4°C the resin was washed with 0.1M sodiumbicarbonate to remove excess antigen. Resin was then capped using 0.1M Tris-HCl buffer (pH8.0) for 2hrs, to block any residual reactive groups. Resin was washed with copious amounts of PBS before use. Rabbit serum was incubated with beads to allow the antibody to bind the antigen for 1hr at room temperature. Resin was washed with PBS to remove unbound protein. Antibody was then eluted from the resin using acidic elution buffer (0.1M Glycine-HCl, pH 2.8). Eluted sample was immediately neutralized using Tris to bring the solution back to physiological pH.

***Constructs:*** RNF26 was amplified from IMAGE: 3507662 and cloned into mRFP-C1, mGFP-C1 and 2HA-C1 vectors by EcoRI/BamH1 restriction sites. Inactive mutants of RNF26 (C401S and I382R) were created by site directed mutagenesis. RFP-RNF26 Tail (aa 246-433) was amplified from the full length construct into mRFP via EcoRI/BamHI Restriction sites. Tollip was cloned into mGFP-C1, 2xHA-C1 and 2xFLAG-C1 by KpnI/HindIII restriction sites. GFP-Tollip M240A/F241A, HA-Tollip M240A/F241A and HA-tagged lysine-mutants were created from the full length construct by site directed mutagenesis. GFP-Tom1L2 was cloned into mGFP-C1 using XhoI/HindIII restriction sites, GFP-Tom1L2 E240A was made from the full length construct by site directed mutagenesis. HA-SQSTM1 was bought from Addgene (#28027), GFP-SQSTM1 was amplified from Addgene plasmid #28027 into mGFP-C1 using EcoRI/XhoI restriction sites. GFP-SQSTM1 M404T was made from the full length construct by site directed mutagenesis. TAX1BP1 was cloned into mGFP-C1 using the restriction enzymes Asp718 and BamHI, GFP-TAX1BP1 F737A and F764A were made from the full length construct by site directed mutagenesis. GFP-EPS15, FLAG-EPS15 and FLAG-EPS15 L883A/L885A in pMT2SM were a gift from J. Borst (NKI, Amsterdam). GFP-Myosin VI NI full length, tail and RRL-AAA/WWL-WLY mutants were generous gift from F. Buss (Cambridge). HA-ubiquitin in pcDNA3.1 was a generous gift from I. Dikic (Institute for Biochemie II, Frankfurt). FLAG-ubiquitin was cloned from HA-ubiquitin into pcDNA3.1+ using EcoRI/BamHI restriction sites. HA-VAPA was a gift from R. van de Kant (NKI, Amsterdam). USE1-GFP was a gift from T. Scanu (NKI, Amsterdam). HA-Tom1 was cloned into 2xHA-C1 using XhoI/HindIII restriction sites. FLAG-DOCK7 was a gift from L. van Aelst (Cold Spring Harbor Laboratory, New York). CD63-mCherry was cloned from CD63-GFP (gift from G. Griffith) by L. Janssen using NheI/BamHI restriction sites.

***Site directed Mutagenesis:*** Forward en reverse primers containing the desired mutations were created. A mixture containing template DNA, 1x Pfu buffer, 20mM dNTPs, 0.6µM forward primer, 0.6µM reverse primer, 1µl Turbo Pfu Polymerase filled to 50µl with DEPC was amplified using the following program: 95˚C 2min; (95˚C 30s; 52˚C 30s; 68˚C 13min + 2min/Kb) x 20 cycles; 68˚C 20min; 4˚C forever. 20µl amplified product was incubated with 2µl DpnI (Thermo scientific) for 4hrs at 37˚C to digest the template DNA. The mutated DNA was transformed into DH5β using 2xYT medium to increase the amount of the mutated constructs.

***siRNA transfection:*** Gene silencing was performed in a 24 well plate using 50µl siRNA (500nM stock) mixed with 0.75µl DharmaFECT1 #1 (Dharmacon) diluted in 49.25µl IMDM. The mixture was incubated for 20min on a shaker followed by the addition of 28,000 MelJuSo cells in IMDM and cultured for three days at 37˚C and 5%CO2 before analysis. Non-targeting siRNA (siCTRL, D-001206-13-20, Dharmacon) was used as a negative control. RNF26 interacting proteins were silenced using siRNAs from the siGenome SMARTpool library (Dharmacon).

| Gene | siRNA sequence (sense) |
|---|---|
| RNF26 #1 (siGENOME D-007060-02) | CGUAGUG-GCUGCCUUCCUA |
| RNF26 #2 (siGENOME D-007060-04) | GCAGAUCAGAGGCA-GAAGA |
| RNF26 #3 (siGENOME D-007060-17) | GAGAGGAUGU-CAUGCGGCU |
| RNF26 3'UTR (Custom, Thermo Sci) | CAGGAGGGAUAAC-CGGAUUUU |
| Myosin VI 5'UTR (Custom, Thermo Sci) | GGAAACAGGA-GAUCGUGGAUU |

***DNA transfections:*** MelJuSo and HeLa cells seeded in a 12-well plate were transfected using Extremegene HP (Roche). 100µl IMDM medium was mixed with 3µl Extremegene HP and 1µg DNA. After 30min, the mix was added to the MelJuSo cells and cultured for one day at 37˚C and 5% CO2 before analysis. HEK293T cells seeded in a 6-well plate were transfected using PEI (Polyethylenimine, 23966, Polysciences Inc.). 100µl IMDM medium was mixed with 6µl PEI and 2µg DNA. After 30min, the mix was added to the HEK293T cells and cultured for one day at 37˚C and 5% CO2 before analysis.

***Confocal Microscopy:*** MelJuso and HeLa cells were fixed with PBS/3.75% formaldehyde (free from acid, Merck), permeabilized with PBS/0.1% TritonX-100 (T8787, Sigma) and blocked with PBS/0.5% bovine serum albumin (BSA, A8022, Sigma). Cell were stained using the desired antibodies diluted in PBS/0.5% bovine serum albumin. Stained cells were analyzed by a Leica SP5 microscope with appropriate filters for fluorescence detection. Pictures were taken using a HCX PL 63x 1.32 oil objective. Hoechst was excited at λ=405nm and detected at λ=416-470nm; Alexa-488 was excited at λ=488nm and detected at λ=500-550nm. Alexa-568 was excited at λ=561nm and detected at λ=570-621 nm; Alexa-647 was excited at λ=633nm and detected at λ=642-742nm.

***qPCR:*** Messenger RNA was extracted from cells using the mRNA Capture Kit (11787896001, Roche) and reverse transcribed into cDNA using the Transcriptor High Fidelity cDNA Synthesis Kit (05081866001, Roche). Quantitative RT-PCR was performed using LightCycler® 480 SYBR Green 1 Master (04707516001, Roche) on the LightCycler® 480 Detection System (Roche). Primer sequences are listed in a table below. Quantification was performed using the comparative CT method

(ΔΔCT). The results were expressed relative to 18S values; normalized to control siRNA treated cells and LOG-transformed.

| Gene | Primer sequence |
|---|---|
| 18S | (5'-3') CGGCTACCACATCCAAGGAA |
| | (3'-5') GCTGGAATTACCGCGGCT |
| RNF26 | (5'-3') TCGGCACTCAGAACCTCTTT |
| | (3'-5') CTAGGAAGGCAGCCACTACG |

***Immunoelectron microscopy.*** MelJuSo cells with GFP-RNF26 were fixed for 2hrs in a mixture of 2%paraformaldehyde and 0.2%glutaraldehyde in 60mM PIPES, 25mM HEPES, 2mM MgCl2, 10mM EGTA, pH6.9 and processed for ultrathin cryosectioning as described [53]. For immunolabelling, the sections were incubated for 10min with 0.15M glycine in PBS and for 1 min with 1%BSA in PBS to block free aldehyde groups and prevent aspecific antibody binding, respectively. Sections were incubated with rabbit anti-PDI (H. Ploegh, MIT, Boston) and 10 nm protein-A conjugated colloidal gold (EMlab, University of Utrecht) all in 1% BSA in PBS. Next, sections were fixed in 1% glutaraldehyde and blocked with glycine and BSA in PBS, followed by rabbit anti-RNF26 and as amplifying step an extra Swine anti-Rabbit Ig followed by 15nm protein-A conjugated gold probe. Next, the cryosections were embedded in uranylacetate and methylcellulose and examined with a Philips CM 10 electron microscope (FEI Eindhoven, The Netherlands).

***GST-pulldown:*** MelJuSo cells were lysed for 30 min in lysis buffer containing 0.8% NP-40 (74385, Sigma), 50mM NaCl, 50mM Tris-HCl pH8.0, 5mM MgCl2, 10% Glycerol, 1mM DTT and phosphatase inhibitors (Roche Diagnostics, EDTA free). Supernatant after spinning (10min at max. speed) was incubated with GST- or GST-RNF26 Tail (aa304-433 and aa363-433) coupled Glutathione-Sepharose beads 4B (GE Healthcare) for 1hr (20µg protein/50µl beads). Beads were washed four times in Wash buffer containing (0.08% NP-40, 250mM NaCl, 50mM Tris-HCl pH 8.0 and 5mM MgCl2) before addition of Laemmli Sample Buffer (containing 5% β-mercaptoethanol) followed by 5min incubation at 95°C. Detection of pulled-down proteins was done by SDS-PAGE followed by silver staining (SilverQuest Silver Staining Kit, LC6070, Invitrogen). Specific bands were analyzed by mass spectrometry.

***Co-immunoprecipitation:*** HEK293T cells were lysed for 30min in lysis buffer containing 0.8% NP-40, 50 mM NaCl, 50 mM Tris-HCl pH8.0, 5mM MgCl2 and phosphatase inhibitors (Roche Diagnostics, EDTA free). Supernatant after spinning (10min at max. speed) was incubated with antibody-coupled Protein G 4 fast flow (GE Healthcare) for 1hr. Beads were washed four times in Wash buffer containing 0.08% NP-40, 150mM NaCl, 50mM Tris-HCl pH 8.0 and 5mM MgCl2 before addition of Laemmli Sample Buffer (containing 5% β-mercaptoethanol) followed by 5min incubation at 95°C. Co-immunoprecipitated proteins were separated by SDS-PAGE, western blotted and detected by antibody staining. Depending on the secondary antibodies used, antibody signals were detected by Chemidoc XRS+ imager (Bio-Rad) or Odyssey imager.

***Ubiquitination-assay:*** HEK293T cells were lysed for 30 min in 0.5%TX100 lysis buffer containing 50mM Tris-HCl pH7.5, 150mM NaCl, 5mM EDTA, 0.5%TX100, freshly added 10mM NMM (DUB inhibitor diluted in DMSO) and protease inhibitors (Roche Diagnostics, EDTA free). Supernatants were frozen at -80°C, thaw and sonicated (Branson Sonifier 250, 3 pulses, Duty Cy-

cle=50%, Output=7). After spinning (10 min at max. speed), we incubated the lysates with antibody-coupled Protein G 4 fast flow (GE Healthcare) for one hour. Beads were washed four times in 0.5%TX100 containing lysis buffer before addition of Laemmli Sample Buffer (containing 5% β-mercaptoethanol) followed by 5 min incubation at 95˚C. Proteins were separated by SDS-PAGE (8% acrylamide gel), transferred to nitrocellulose membranes and detected with antibodies. Li-Cor fluorescent dyes were used as secondary antibodies and detected by an Odyssey Classic imager (Li-Cor).

***SDS-PAGE and Western blotting:*** Samples were separated by a 10% acrylamide gel and transferred to a nitrocellulose membrane (Protan BA85, 0.45µm, GE Healthcare) or PVDF membrane (Immobilon-P, 0.45µm, Millipore) at 300mA for 2hrs. The filters were blocked in PBS/0.1%Tween20 (P1379, Sigma-Aldrich)/5% Milk (Skim milk powder, LP0031, Oxiod) (Note: nitrocellulose membranes used for Odyssey readouts were blocked in PBS/5%Milk without Tween to reduce background) and incubated with a primary antibody for 1hr diluted in PBS/0.1%Tween/5% Milk, washed 3x 10min in PBS/0.1% Tween and incubated with the secondary antibody for 45min diluted in PBS/0.1%Tween/5% Milk and washed 3x in PBS/0.1% Tween. Depending on the secondary antibody, the blot was incubated with ECL reagent (SuperSignal West Dura Extended Duration Substrate, Thermo Scientific) and the signal was detected using the Chemidoc XRS+ imager (Bio-Rad) or directly imaged by the Odyssey Classic imager (Li-Cor).

***Life Cell Imaging:*** MelJuSo cells were depleted for RNF26 using siRNAs and grown in Willco wells (HBSt-3522). Two days post-transfection, the cells were imaged overnight on a Zeiss CCD5 microscope (Observer. Z1) using a 40x objective. The time between rounding up of the cell and separation of the daughter cells was determined. For statistical analysis, p-values were determined using the Student's t test.

**Reference List**

1 Ross,J.L. et al. (2008) Cargo transport: molecular motors navigate a complex cytoskeleton. Curr. Opin. Cell Biol. 20, 41-47

2 Johansson,M. et al. (2007) Activation of endosomal dynein motors by stepwise assembly of Rab7-RILP-p150Glued, ORP1L, and the receptor betalll spectrin. J. Cell Biol. 176, 459-471

3 Rocha,N. et al. (2009) Cholesterol sensor ORP1L contacts the ER protein VAP to control Rab7-RILP-p150 Glued and late endosome positioning. J. Cell Biol. 185, 1209-1225

4 Helle,S.C. et al. (2013) Organization and function of membrane contact sites. Biochim. Biophys. Acta 1833, 2526-2541

5 van der Kant,R. and Neefjes,J. (2014) Small regulators, major consequences - Ca(2)(+) and cholesterol at the endosome-ER interface. J. Cell Sci. 127, 929-938

6 Gould,G.W. and Lippincott-Schwartz,J. (2009) New roles for endosomes: from vesicular carriers to multi-purpose platforms. Nat. Rev. Mol. Cell Biol. 10, 287-292

7 Paul,P. et al. (2011) A Genome-wide multidimensional RNAi screen reveals pathways controlling MHC class II antigen presentation. Cell 145, 268-283

8 Wells,A.L. et al. (1999) Myosin VI is an actin-based motor that moves backwards. Nature 401, 505-508

9 Inoue,A. et al. (2002) DOC-2/DAB2 is the binding partner of myosin VI. Biochem. Biophys. Res. Commun. 292, 300-307

10 Morris,S.M. et al. (2002) Myosin VI binds to and localises with Dab2, potentially linking receptor-mediated endocytosis and the actin cytoskeleton. Traffic. 3, 331-341

11 Spudich,G. et al. (2007) Myosin VI targeting to clathrin-coated structures and dimerization is mediated by binding to Disabled-2 and PtdIns(4,5)P2. Nat Cell Biol 9, 176-183

12 Bunn,R.C. et al. (1999) Protein interactions with the glucose transporter binding protein GLUT1CBP that provide a link between GLUT1 and the cytoskeleton. Mol. Biol. Cell 10, 819-832

13 Tumbarello,D.A. et al. (2012) Autophagy receptors link myosin VI to autophagosomes to mediate Tom1-dependent autophagosome maturation and fusion with the lysosome. Nat Cell Biol 14, 1024-1035

14 Arden,S.D. et al. (2007) Myosin VI is required for targeted membrane transport during cytokinesis. Mol. Biol. Cell 18, 4750-4761

15 Finan,D. et al. (2011) Proteomics approach to study the functions of Drosophila myosin VI through identification of multiple cargo-binding proteins. Proc Natl Acad Sci U S A 108, 5566-5571

16 Morriswood,B. et al. (2007) T6BP and NDP52 are myosin VI binding partners with potential roles in cytokine signalling and cell adhesion. J Cell Sci 120, 2574-2585

17 Majewski,L. et al. (2012) Dock7: a GEF for Rho-family GTPases and a novel myosin VI-binding partner in neuronal PC12 cells. Biochem Cell Biol 90, 565-574

18 Deshaies,R.J. and Joazeiro,C.A. (2009) RING domain E3 ubiquitin ligases. Annu Rev Biochem 78, 399-434

19 Lippai,M. and Low,P. (2014) The Role of the Selective Adaptor p62 and Ubiquitin-Like Proteins in Autophagy. Biomed. Res. Int. 2014, 832704

20 Zhang,J. et al. (2012) Rabs and EHDs: alternate modes for traffic control. Biosci. Rep. 32, 17-23

21 Katoh,Y. et al. (2006) Recruitment of clathrin onto endosomes by the Tom1-Tollip complex. Biochem Biophys Res Commun 341, 143-149

22 Katoh,Y. et al. (2004) Tollip and Tom1 form a complex and recruit ubiquitin-conjugated proteins onto early endosomes. J. Biol. Chem. 279, 24435-24443

23 Tumbarello,D.A. et al. (2013) Myosin VI and its cargo adaptors - linking endocytosis and autophagy. J. Cell Sci. 126, 2561-2570

24 Smith,C.M. and Chircop,M. (2012) Clathrin-mediated endocytic proteins are involved in regulating mitotic progression and completion. Traffic 13, 1628-1641

25 Husnjak,K. and Dikic,I. (2012) Ubiquitin-binding proteins: decoders of ubiquitin-mediated cellular functions. Annu. Rev. Biochem. 81, 291-322

26 Penengo,L. et al. (2006) Crystal structure of the ubiquitin binding domains of rabex-5 reveals two modes of interaction with ubiquitin. Cell 124, 1183-1195

27 Cote,J.F. and Vuori,K. (2002) Identification of an evolutionarily conserved superfamily of DOCK180-related proteins with guanine nucleotide exchange activity. J. Cell Sci. 115, 4901-4913

28 Menendez-Benito,V. et al. (2013) Spatiotemporal analysis of organelle and macromolecular complex inheritance. Proc. Natl. Acad. Sci. U. S. A 110, 175-180

29 Schiel,J.A. and Prekeris,R. (2013) Membrane dynamics during cytokinesis. Curr. Opin. Cell Biol. 25, 92-98

30 Chen,C.T. et al. (2012) Orchestrating vesicle transport, ESCRTs and kinase surveillance during abscission. Nat. Rev. Mol. Cell Biol. 13, 483-488

31 Wang,T. et al. (2010) The emerging role of VHS domain-containing Tom1, Tom1L1 and Tom1L2 in membrane trafficking. Traffic. 11, 1119-1128

32 Ankem,G. et al. (2011) The C2 domain of Tollip, a Toll-like receptor signalling regulator, exhibits broad preference for phosphoinositides. Biochem. J. 435, 597-608

33 Chi,S. et al. (2008) Eps15 mediates vesicle trafficking from the trans-Golgi network via an interaction with the clathrin adaptor AP-1. Mol Biol Cell 19, 3564-3575

34 Hurley,J.H. et al. (2006) Ubiquitin-binding domains. Biochem. J. 399, 361-372

35 Bilodeau,P.S. et al. (2004) The GAT domains of clathrin-associated GGA proteins have two ubiquitin binding motifs. J. Biol. Chem. 279, 54808-54816

36 Hirano,S. et al. (2006) Double-sided ubiquitin binding of Hrs-UIM in endosomal protein sorting. Nat. Struct. Mol. Biol. 13, 272-277

37 Lenk,U. et al. (2002) A role for mammalian Ubc6 homologues in ER-associated protein degradation. J. Cell Sci. 115, 3007-3014

38 Rock,R.S. et al. (2005) A flexible domain is essential for the large step size and proces-

sivity of myosin VI. Mol. Cell 17, 603-609

39 Lister,I. et al. (2004) A monomeric myosin VI with a large working stroke. EMBO J. 23, 1729-1738

40 Bond,L.M. et al. (2012) Dynamic exchange of myosin VI on endocytic structures. J. Biol. Chem. 287, 38637-38646

41 Park,H. et al. (2006) Full-length myosin VI dimerizes and moves processively along actin filaments upon monomer clustering. Mol. Cell 21, 331-336

42 Phichith,D. et al. (2009) Cargo binding induces dimerization of myosin VI. Proc. Natl. Acad. Sci. U. S. A 106, 17320-17324

43 Yu,C. et al. (2009) Myosin VI undergoes cargo-mediated dimerization. Cell 138, 537-548

44 Prag,G. et al. (2003) Mechanism of ubiquitin recognition by the CUE domain of Vps9p. Cell 113, 609-620

45 Buss,F. et al. (2004) Myosin VI: cellular functions and motor properties. Annu. Rev. Cell Dev. Biol. 20, 649-676

46 Frank,D.J. et al. (2004) Myosin VI: a structural role in actin organization important for protein and organelle localization and trafficking. Curr. Opin. Cell Biol. 16, 189-194

47 Loubery,S. et al. (2012) Myosin VI regulates actin dynamics and melanosome biogenesis. Traffic. 13, 665-680

48 Birgisdottir,A.B. et al. (2013) The LIR motif - crucial for selective autophagy. J. Cell Sci. 126, 3237-3247

49 Schweitzer,J.K. et al. (2005) Endocytosis resumes during late mitosis and is required for cytokinesis. J. Biol. Chem. 280, 41628-41635

50 McLean,J.R. et al. (2011) Survey of the phosphorylation status of the Schizosaccharomyces pombe deubiquitinating enzyme (DUB) family. J. Proteome. Res. 10, 1208-1215

51 Neefjes,J.J. et al. (1990) The biosynthetic pathway of MHC class II but not class I molecules intersects the endocytic route. Cell 61, 171-183

52 Vennegoor,C. and Rumke,P. (1986) Circulating melanoma-associated antigen detected by monoclonal antibody NKI/C-3. Cancer Immunol. Immunother. 23, 93-100

53 Calafat,J. et al. (1997) Human monocytes and neutrophils store transforming growth factor-alpha in a subpopulation of cytoplasmic granules. Blood 90, 1255-1266

# Supplemental Figures
# Chapter 4

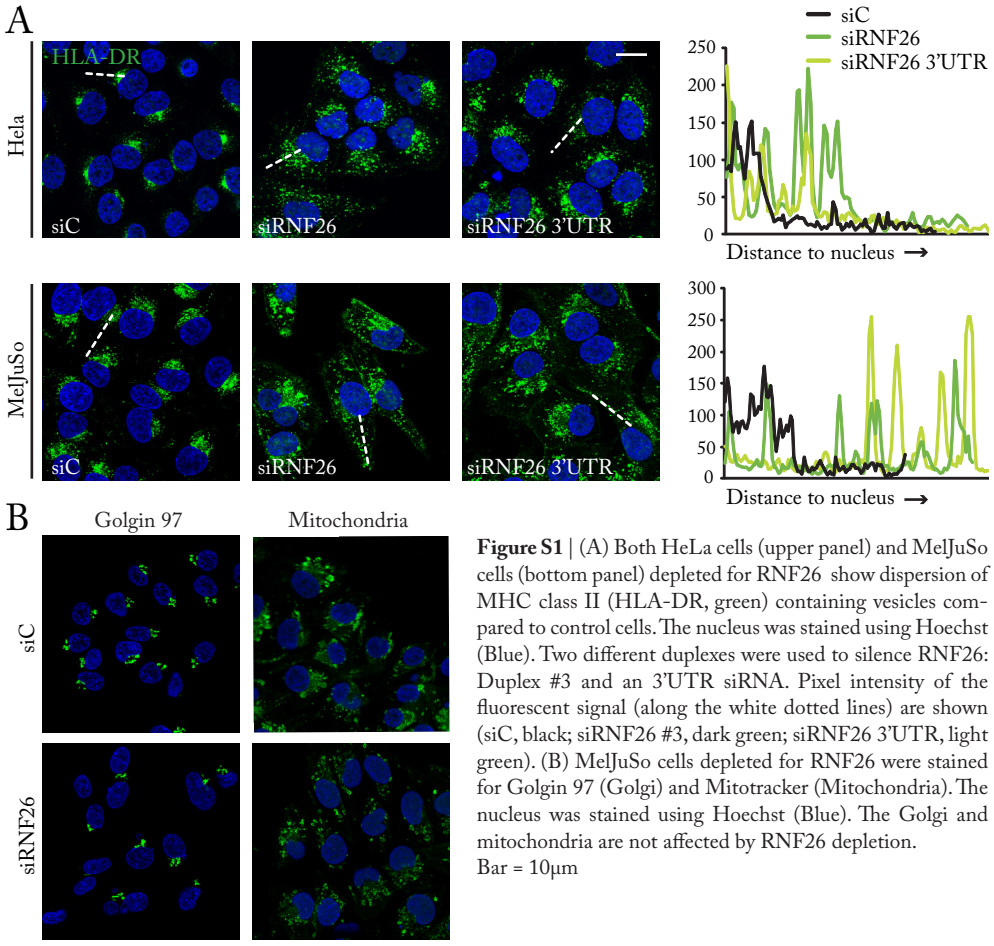


**Figure S1** | (A) Both HeLa cells (upper panel) and MelJuSo cells (bottom panel) depleted for RNF26 show dispersion of MHC class II (HLA-DR, green) containing vesicles compared to control cells. The nucleus was stained using Hoechst (Blue). Two different duplexes were used to silence RNF26: Duplex #3 and an 3'UTR siRNA. Pixel intensity of the fluorescent signal (along the white dotted lines) are shown (siC, black; siRNF26 #3, dark green; siRNF26 3'UTR, light green). (B) MelJuSo cells depleted for RNF26 were stained for Golgin 97 (Golgi) and Mitotracker (Mitochondria). The nucleus was stained using Hoechst (Blue). The Golgi and mitochondria are not affected by RNF26 depletion.
Bar = 10μm

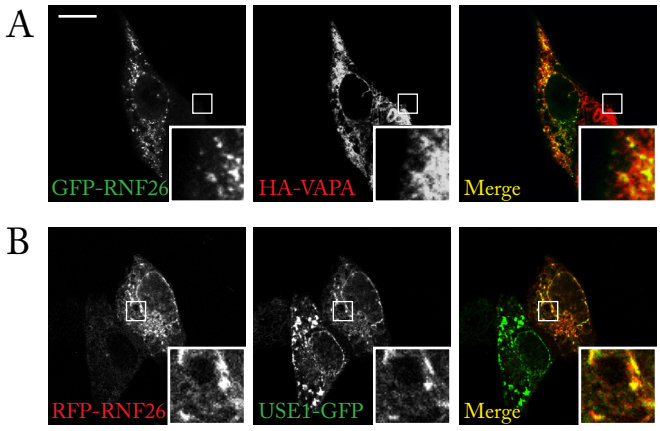


**Figure S2** | (A) MelJuSo cells overexpressing GFP-RNF26 (green) and the ER membrane protein HA-VAPA (red) show co-localization in the ER membrane (yellow). (B) MelJuSo cells over-expressing RFP-RNF26 (red) and the ER membrane protein USE1-GFP (green) show co-localization in the ER membrane (yellow).
Bar = 10μm

A

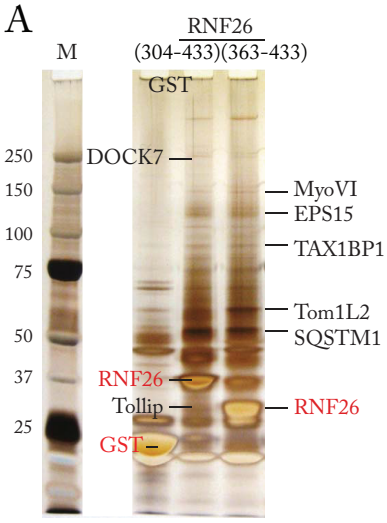


**Figure S3** | (A) Pulldown samples using GST-RNF26 Tail (aa304-433), GST-RNF26 RING (aa363-433) or GST coated beads incubated with MelJuSo lysate were separated by SDS-PAGE and silver stained. Specific bands were analyzed by mass spectrometry. Areas containing the seven proteins involved in endosomal localization are marked. Molecular weight standard is indicated. (B) Complete list of by pulldown and mass spectrometry identified potential RNF26 interacting proteins.

B

| Gene ID | # pts found by MS | Size (kD) | Domains | Localization | Ontology process | Function |
|---|---|---|---|---|---|---|
| HUWE1 | 103 | 482 | HECT/UBA/WWE | Nucleus, Cytosol | Ubiquitin cycle, Polyubiquitination | E3 ligase |
| MYO6 | 41 | 145 | MYSc | Unconventional Myosin | Actin-filament based movement | Motor protein |
| RNF31 | 26 | 120 | 2xRING/3xZnF/PUB | | | E3 ligase |
| TAX1BP1 | 23 | 86 | 2xZnF | Intracellular | Apoptosis | |
| SQSTM1 | 20 | 48 | PB1/ZnF/UBA | Nucleus, Cytosol | Immune respons, apoptosis, respons to stress | Adapter protein, binds Ub |
| RBCK1 | 19 | 58 | RING/ZnF | Intracellular | Ubiquitin cycle | E3 ligase |
| HSPA5 | 18 | 78 | Signal pt | Nucleus, ER lumen | anti-apoptosis | Heat shock protein |
| VIM | 16 | 54 | | Cytoskeleton | Cell motility | Intermediate filament |
| SOLH | 15 | 117 | 5xZnF/CysPc | Intracellular | | |
| KEAP1 | 9 | 70 | ZnF (BTB and BACK) | | Transcription | Adaptor protein |
| TOM1L2 | 8 | 56 | VHS/GAT | Intracellular | Intracellular protein transport | Protein transport |
| USP15 | 6 | 112 | DUSP/UCH | | Ubiquitin-dependent protein catabolism | Peptidase |
| EPS15 | 5 | 99 | 3xUIM/EF-hands | PM, Coated-pit | Vesicle organisation and biogenesis | Assembly of clathrin-coated pits |
| TOLLIP | 5 | 30 | C2/CUE | IL-18 receptor complex | Intracellular signalling cascade | |
| SIPL1 | 4 | 34 | ZnF | Intracellular | | |
| MAP7D2 | 3 | 86 | MAP7 | | | Microtubule associated protein |
| CCDC50 | 2 | 56 | | | | Involved in EGFR signaling |
| DOCK7 | 2 | 241 | | | | Guanine Exchange Factor (GEF) |

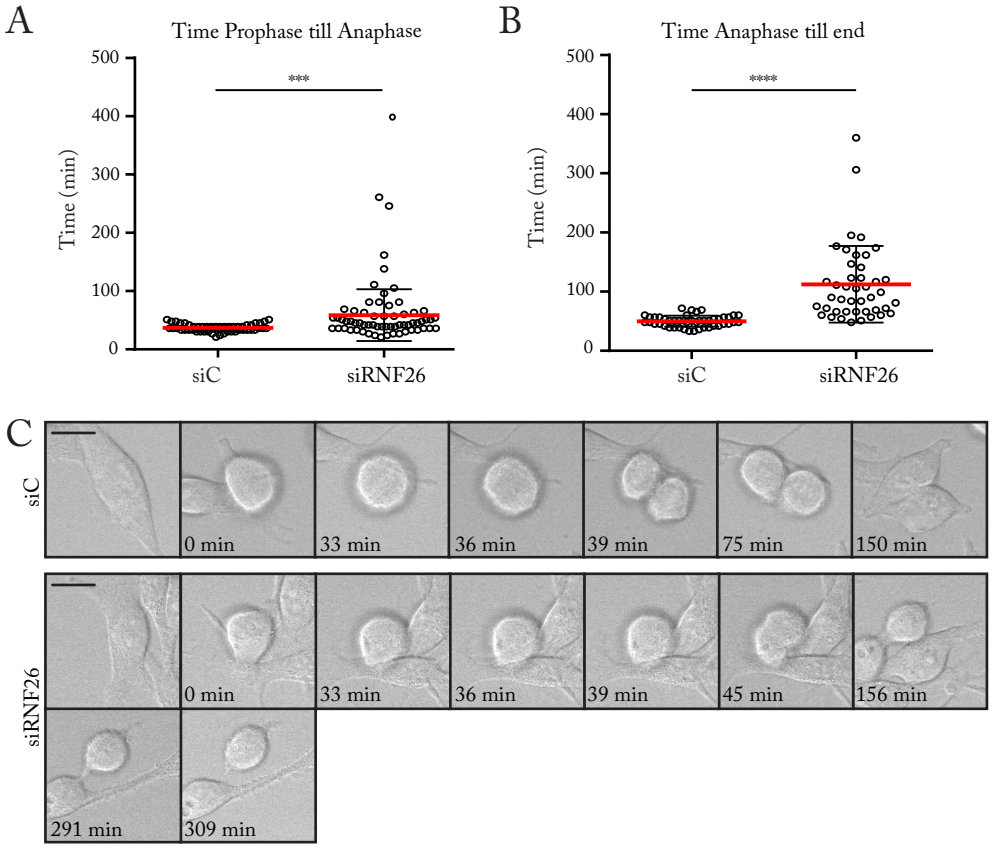


**Figure S4** | RNF26 depleted cells and cells treated with a non-targeting siRNA were followed during their cell cycles. (A) Time between the start of mitosis (when the cell rounds up) and the onset of anaphase was determined for both conditions. RNF26 depletion only slightly increases the duration of the first steps of mitosis (siRNF26 50min; siC 40min). (B) Time between anaphase onset and the end of the cell cycle was determined. The duration of the last step in mitosis, daughter cell separation during cytokinesis, was clearly elongated (siRNF26 110min; siC 50min). (C) Still images of the different phases of the cell cycle in RNF26 depleted and control cells with indicated time-points. Bar = 10μm, ***p< 0.0005, ****p<0.0001